Fundamentals of Electrochemistry

References

Electrochemical Methods : Fundamentals and Applications, 2nd edition.
by A. J. Bard and L.R. Faulkner

- Makes use of electrochemistry for the purpose of analysis
- A voltage (potentiometry) or current (voltammetry) signal originating from an electrochemical cell is related to the activity or concentration of a particular species in the cell.
- Excellent detection limit (10^{-8} ~ 10^{-3} M):

  1959, Nobel Prize (Polarography)
- Inexpensive technique.
- Easily miniaturized : implantable and/or portable (biosensor, biochip)

Electrochemical cells

Galvanic cell

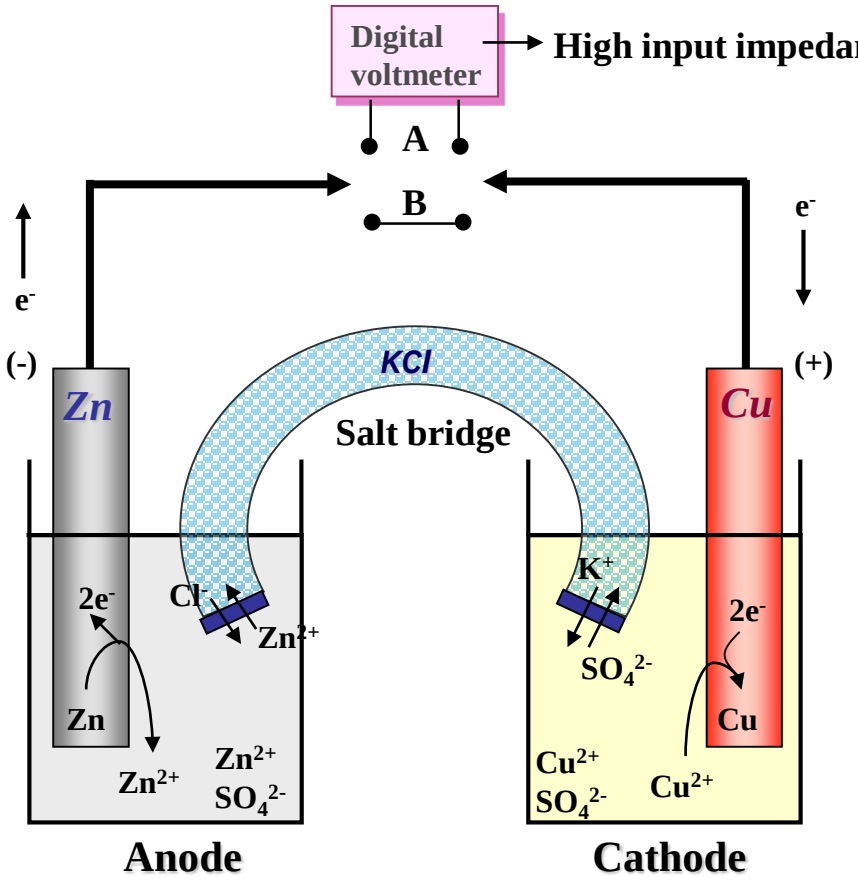

Anode reaction : oxidation

$$Zn \rightleftharpoons Zn^{2+} + 2e^-$$

Cathode reaction : reduction

$$Cu^{2+} + 2e^- \rightleftharpoons Cu$$

$$Zn + Cu^{2+} \rightleftharpoons Zn^{2+} + Cu$$

- **Cell potential** : a measure of difference in electron energy between the two electrodes
- **Open-circuit potential (zero-current potential)** : can be calculated from thermodynamic data, ie. standard cell potentials of the half-cell reactions.

Fig. 27.1 Electrochemical cell consisting of a zinc electrode in 0.1 M $ZnSO_4$, a copper electrode in 0.1 M $CuSO_4$, and a salt bridge. Galvanic cell. (From Heineman book)

Standard Electrode Potential

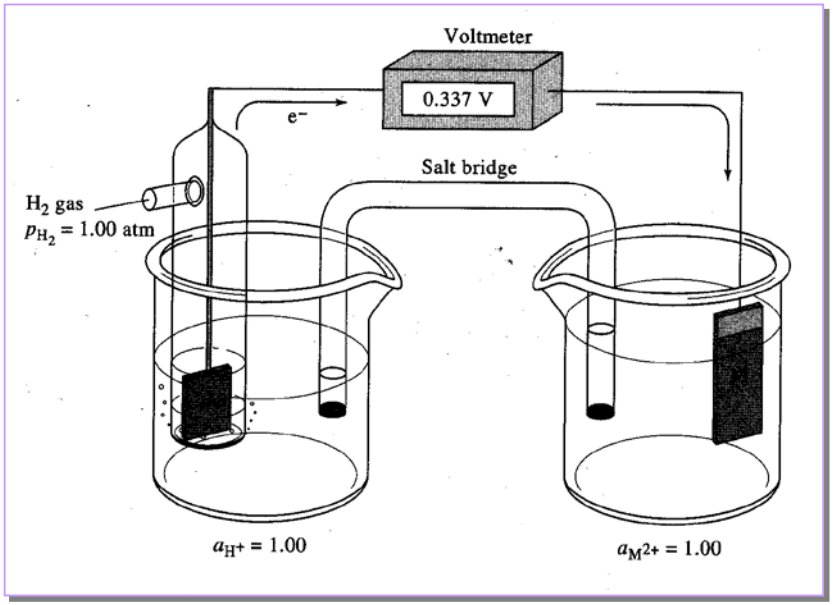

- A quantitative description of the relative driving force for a half-cell reaction.
- A relative quantity vs standard hydrogen electron assigned to zero volt. E^0(SHE)=0

Fig. 22.5 Definition of the standard electrode potential for $M^{2+}(aq) + 2e^- \rightleftharpoons M(s)$.

Table 22.1 Standard Electrode Potentials

Reaction	E^0 at 25 °C, V
$Cl_2(g) + 2e^- \rightarrow 2Cl^-$	+1.359
$O_2(g) + 4H^+ + 4e^- \rightarrow 2H_2O$	+1.229
$Br_2(aq) + 2e^- \rightarrow 2Br^-$	+1.087
$Br_2(l) + 2e^- \rightarrow 2Br^-$	+1.065
$Ag^+ + e^- \rightarrow Ag(s)$	+-.799
$Fe^{3+} + e^- \rightarrow Fe^{2+}$	+0.771
$I_3^- + 2e^- \rightarrow 3I^-$	+0.536
$Cu^{2+} + 2e^- \rightarrow Cu(s)$	+0.337
$Hg_2Cl_2(s) + 2e^- \rightarrow 2Hg(l) + 2Cl^-$	+0.268
$AgCl(s) + e^- \rightarrow Ag(s) + Cl^-$	+0.222
$Ag(S_2O_3)_2^{3-} + e^- \rightarrow Ag(s) + 2S_2O_3^{2-}$	+0.010
$2H^+ + 2e^- \rightarrow H_2(g)$	0.000
$AgI(s) + e^- \rightarrow Ag(s) + I^-$	-0.151
$PbSO_4(s) + 2e^- \rightarrow Pb(S) + SO_4^{2-}$	-0.350
$Cd^{2+} + 2e^- \rightarrow Cd(s)$	-0.403
$Zn^{2+} + 2e^- \rightarrow Zn(s)$	-0.763

Reduction 자발적

SHE

Oxidation 자발적

Nernst Equation (activities of all species = 1)

- **Le Chatelier's principle:**
  increasing reactant concentrations drives the reaction to the right
- **The net driving force of the reaction is expressed by the Nernst equation**
- **The Nernst equation tells us**

the potential of a cell whose reagents are not all unit activity

Nernst Equation for a Half-Reaction

aA + ne$^-$ ⇌ bB

R: gas constant = 8.314 J/Kmol
T: temperature (*K*)

$$E = E^o - \frac{RT}{nF} \ln \frac{A_B^b}{A_A^a}$$

------- (14.13)

$\Delta G = \Delta G^o + RT \ln Q$ (Q; reaction quotient)

$-nFE = -nFE^o + RT \ln Q$ (양변을 nF 로 나누어 준다)

$E = E^o - (RT/nF) \ln Q$

E^o and Equilibrium Constant

- **A galvanic cell produces electricity because the cell reaction is not at equilibrium**
- **The potentiometer allows negligible current to flow**

→The concentration in each half-cell remains unchanged

0.412 V
At the outset

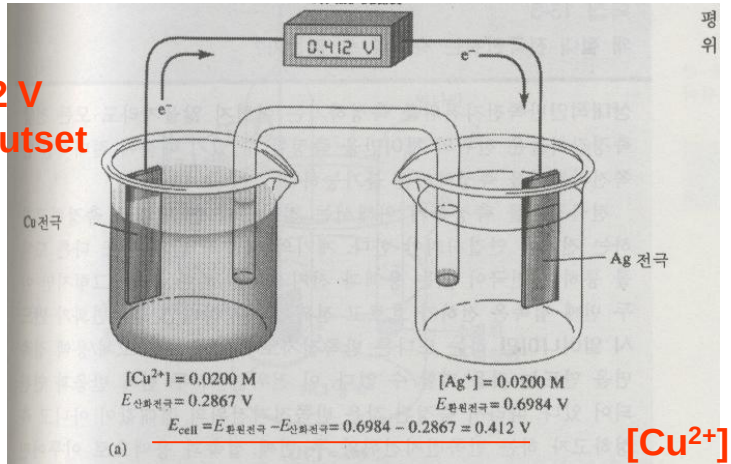

0 V
At equilibrium

[Cu^{2+}] 증가
[Ag^{+}] 감소

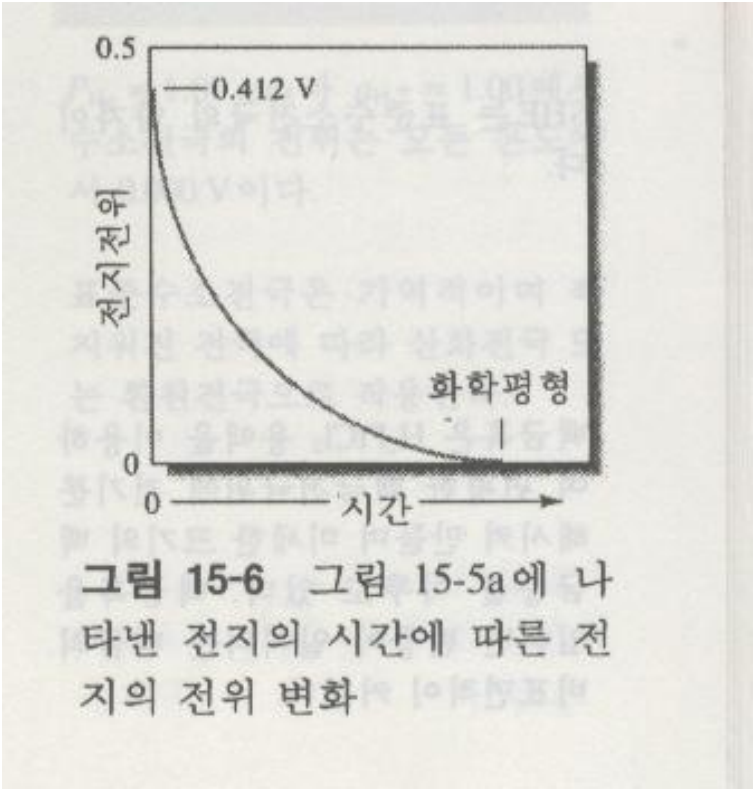

그림 15-6 그림 15-5a에 나타낸 전지의 시간에 따른 전지의 전위 변화

Concentrations in the Operating Cell

A high-quality pH meter (voltmeter) → Resistance = 10^{13} Ω

If we measure 50 mV for Cd^{2+} containing electrochemical cell

Current = E/R = 0.05V/10^{13} Ω = 5 x 10^{-15} A

(5 x 10^{-15} C/s)/(9.649 x10^{4} C/mol) = 5 x 10^{-20} mol e^-/s

The production rate of Cd^{2+} = 2.5 x 10^{-20} mol/s ; negligible concentration change

If we replace the potentiometer with a wire, much more current would flow

→ Concentrations would change until the cell reach equilibrium

Liquid Junction Potential (E_{lj})

E_{lj} (diffusion potential)

- Develops at the interface between two liquids as a result of differences in the rates with which ions move from one liquid to the other.

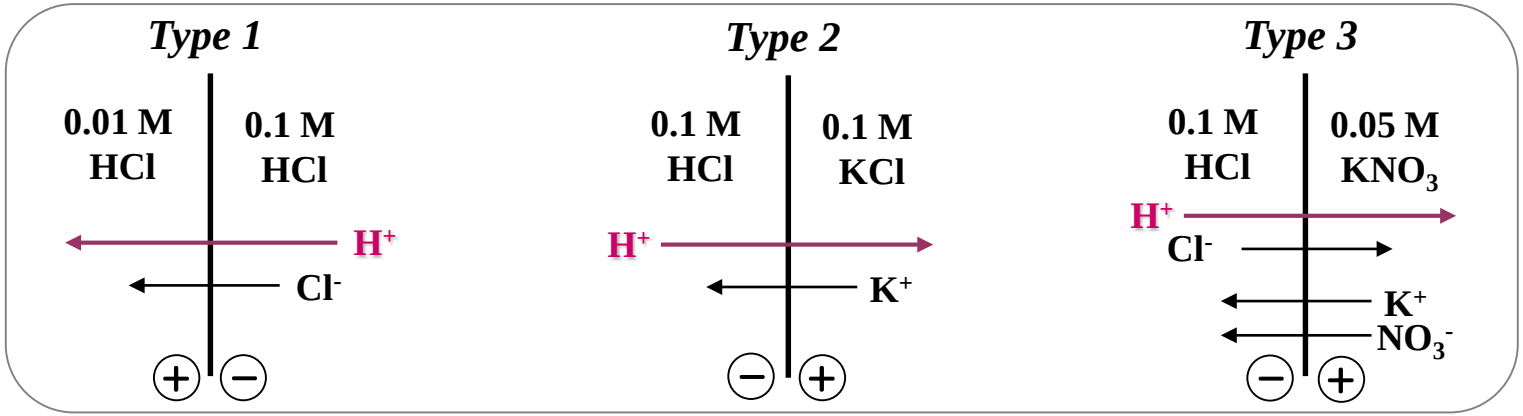

Fig. 27.4 Types of liquid junction. Arrows show the direction of net transfer for each ion, and their lengths indicate relative mobilities. The polarity of the junction potential is indicated in each case by the circled signs.

Table 27.4 Liquid Junction Potentials of 0.1 M Concentrations of Electrolytes

Junction	E_{lj} observed (mV)	Junction	E_{lj} observed (mV)	Junction	E_{lj} observed (mV)	Junction	E_{lj} observed (mV)
HCl : KCl	26.78	HCl : NH_4Cl	28.40	KCl : NH_4Cl	2.16	NaCl : NH_4Cl	-4.21
HCl : NaCl	33.09	KCl : LiCl	8.79	NaCl : LiCl	2.62	LiCl : NH_4Cl	-6.93
KCl : LiCl	34.86	KCl : NaCl	6.42				

Cell Potential

$$E_{cell} = E_{right} - E_{left} + E_{lj} - E_{iR}$$

$E_{right} = E_{cathod}$

$E_{left} = E_{anode}$

Elj = *liquid junction potential*

E_{iR} = *Ohmic loss (iR drop)*

: The potential of an EC cell when electrolysis occurring is diminished by resistance of the cell to current.

Electrochemical cells

Electrolytic cell

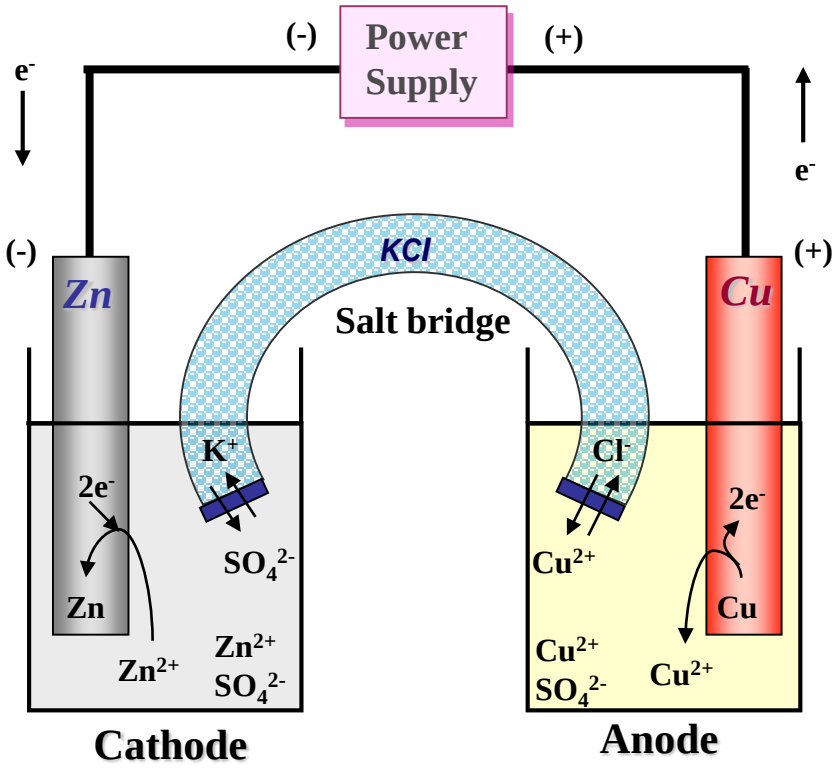

Anode reaction : oxidation

$$Cu \rightleftharpoons Cu^{2+} + 2e^-$$

Cathode reaction : reduction

$$Zn^{2+} + 2e^- \rightleftharpoons Zn$$

$$Cu + Zn^{2+} \rightleftharpoons Cu^{2+} + Zn$$

Fig. 27.1 Electrochemical cell consisting of a zinc electrode in 0.1 M $ZnSO_4$, a copper electrode in 0.1 M $CuSO_4$, and a salt bridge. Electrolytic cell.

Reduction and oxidation process

- We observe or control the potential of the working electrode with respect to the reference.
  → Controlling the energy of the electrons within the working electrode.

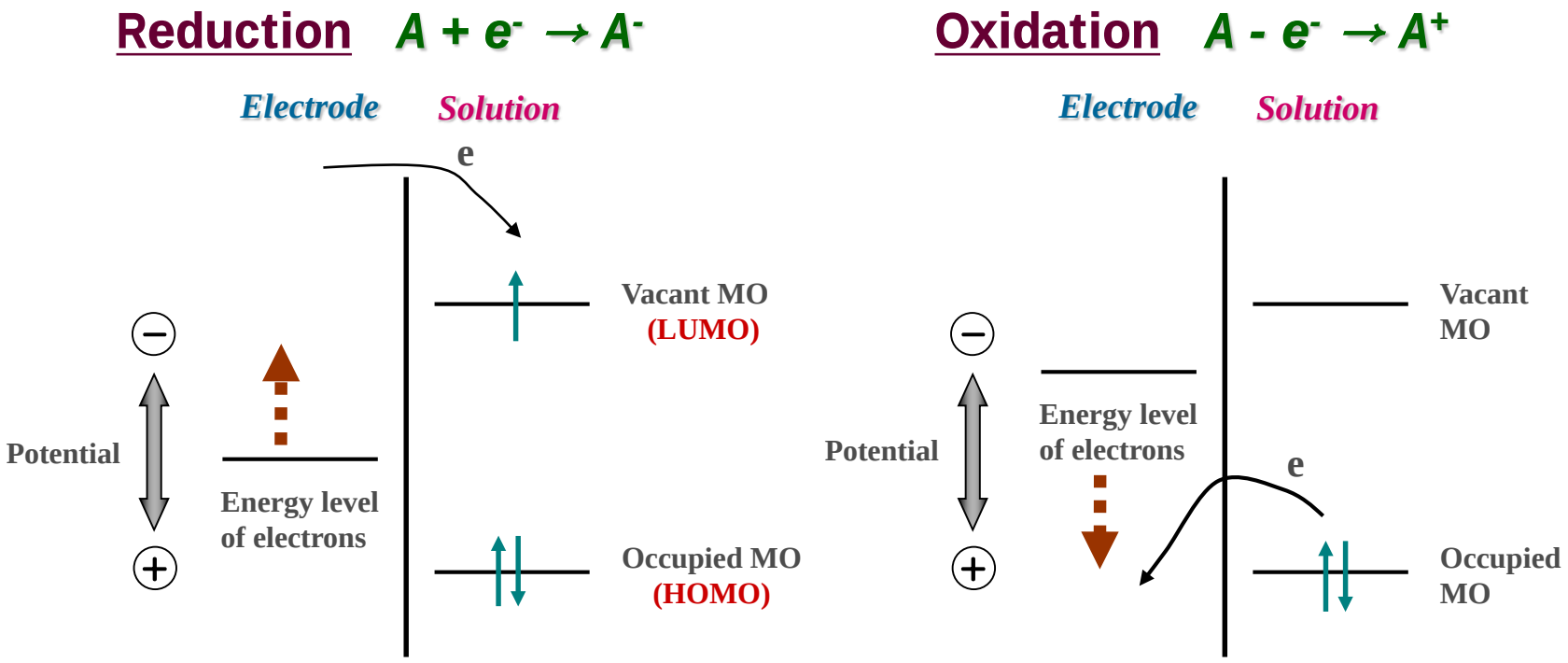

- The critical potentials at which these processes occur are related to the **Standard Potentials, E^0,** for the specific chemical substances in the system.

Determination of HOMO-LUMO Band Gap Energy

- **Use of cyclic voltammetry (CV) or differential pulse voltammetry (DPV)**
- **UV absorption spectrum**
- **Photoluminescence spectrum**

Chem. Mater. **2002,** *14,* 3339−3342

Electrochemical Investigations on PPV Model Compounds

M. Leuze, M. Hohloch, and M. Hanack*

Institut für Organische Chemie, Universität Tübingen, Auf der Morgenstelle 18, D-72076 Tübingen, Germany

Received October 5, 2001. Revised Manuscript Received April 2, 2002

To obtain more information on the redox behavior of poly(*para*-phenylenevinylene) (PPV) and its derivatives, electrochemical investigations were carried out on the short-chain PPV model compounds **1**−**6**. The effects of different substituents were investigated by determinations of the redox potentials by cyclic voltammetry.

Determination of HOMO-LUMO Band Gap Energy

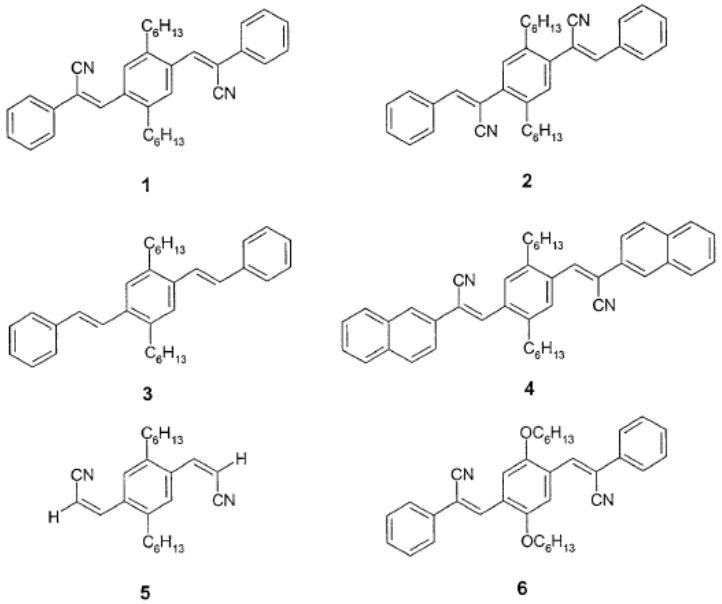

Table 1. Redox Potentials $E_{1/2}$ of 1,4-Bis(2-cyano-2-phenylethenyl)-2,5-dihexylbenzene (1) Determined by Cyclic Voltammetry[a]

solvent	$E_{1/2}(Ox_1)$ (V) (ΔE_p [mV])	$E_{1/2}(Red_1)$ (V) (ΔE_p [mV])	$E_{1/2}(Red_2)$ (V) (ΔE_p [mV])	$E_{1/2}(Red_3)$ (V) (ΔE_p [mV])	$E_{1/2}(Red_4)$ (V) (ΔE_p [mV])
dichloromethane	1.87 (160)	−1.31 (315)	−1.39 (100)		
tetrahydrofuran		−1.27 (135)	−1.43 (120)	−1.66 (95)	−2.11[c]

[a] Scan rate = 100 mV/s. [b] $\Delta E_p = |E_{pa} - E_{pc}|$. [c] Cathodic peak only.

3.18 eV

Table 2. Redox Potentials $E_{1/2}$ of 2 Determined by Cyclic Voltammetry in Different Solvents[a]

solvent	$E_{1/2}(Ox_1)$ (V) (ΔE_p [mV])	$E_{1/2}(Red_1)$ (V) (ΔE_p [mV])	$E_{1/2}(Red_2)$ (V) (ΔE_p [mV])	$E_{1/2}(Red_3)$ (V) (ΔE_p [mV])
dichloromethane	1.98 (70)	−1.61 (130)	−1.66 (240)	
acetonitrile	1.98 (220)	−1.61 (120)	−1.66 (145)	−1.90 (160)
tetrahydrofuran		−1.58 (140)	−1.72 (100)	−1.94 (200)

[a] Scan rate = 100 mV/s.

3.59 eV

Definition of words (What is current?)

Faraday's law

- relate the amount of electrical charge passed through an electrochemical cell to the quantity of material that has undergone electrolysis

$$Q = n\,F\,N \quad \text{..... (1.3.1)}$$

F : faraday constant (96,485 C/mol)

N : the number of moles electrolyzed

n : the number of electrons involved in the electrode or redox reaction

$$i = \frac{dQ}{dt} = nF\frac{dN}{dt} \quad \text{..... (1.3.3)}$$

rearrangement of 1.3.3

$$\textit{Rate (mol/s)} = \frac{dN}{dt} = \frac{i}{nF}$$

Potentiometry

Measurement of cell voltages

Chemical information (activity)

Potentiometry

- Measurement of the difference in potential between the two electrodes of a galvanic cell under the condition of zero current **are described by the term potentiometry**
- **Equilibrium Method**
- Accurate measurements of (a) activities or concentration (b) free-energy change and equilibrium constants of many solution reactions

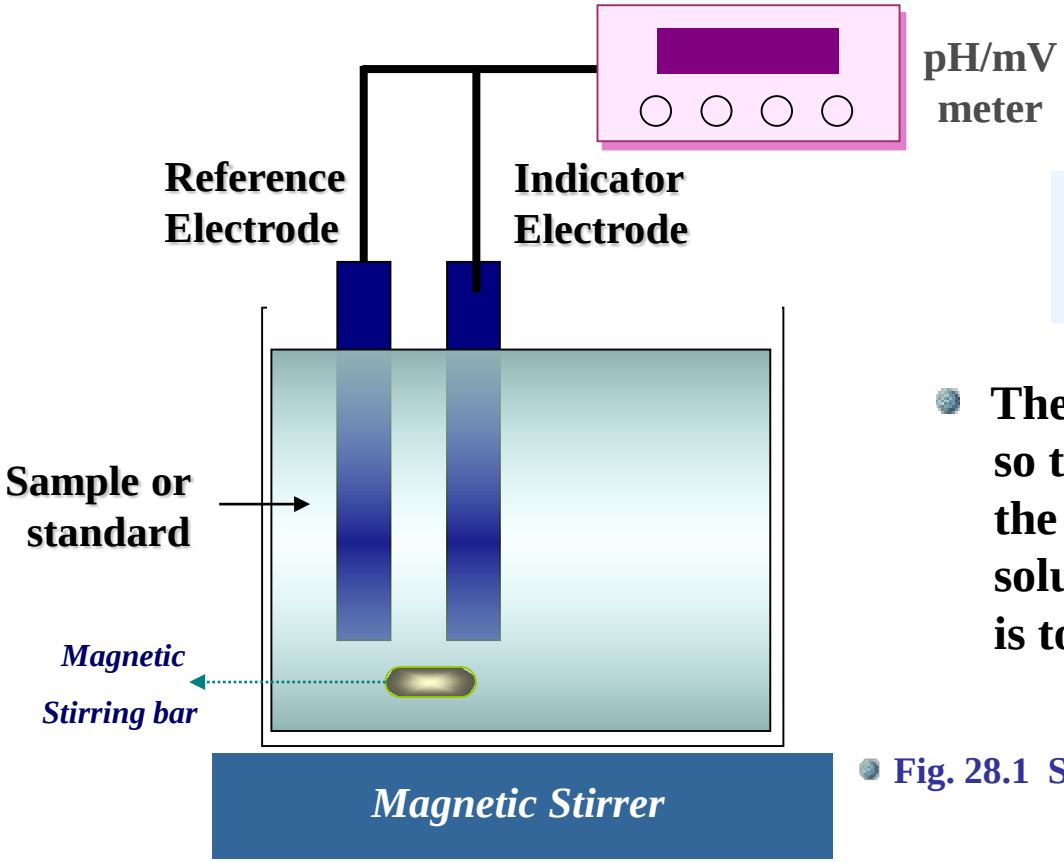

$$E_{cell} = E_{ind} - E_{ref} + E_{lj}$$

- **The indicator electrode is chosen so that its half-cell potential responds to the activity of a particular species in solution whose activity or concentration is to be measured**

- **Fig. 28.1 Schematic diagram of apparatus for potentiometry.**

Electrode and Potentiometry

- **Reference Electrodes : provides a constant potential**

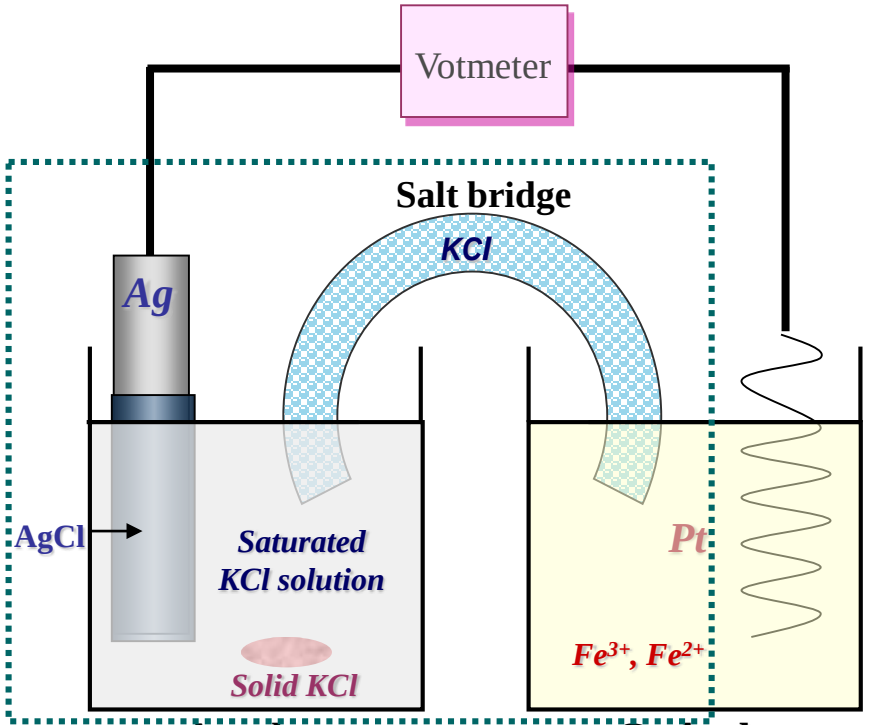

Ag + Cl⁻ ↔ AgCl +e⁻ $Fe^{3+}+e^- \leftrightarrow Fe^{2+}$

$Ag(s)/AgCl(s)/Cl\text{-}(aq)//Fe^{3+}+e^- \leftrightarrow Fe^{2+}(aq)/Pt(s)$

Reference Electrode : $Ag + Cl^- \rightarrow AgCl(s) + e^-$

Anode : $E_-^\circ = 0.222$ V

Indicator Electrode (Pt) : $Fe^{3+} + e^- \rightarrow Fe^{2+}$

Cathode : $E_+^\circ = 0.771$ V

$E_+ = 0.771 - 0.0592 \log[Fe^{2+}]/[Fe^{3+}]$

$E_- = 0.222 - 0.0592 \log[Cl^-]$ *variable*

$E = E_+ - E_- = (0.771 - 0.0592 \log[Fe^{2+}]/[Fe^{3+}]) - (0.222 - 0.0592 \log[Cl^-])$

Measured voltage

Constant ; depend on KCl solubility saturated solution

- **Fig. 15.1 A galvanic cell that can be used to measure the quotient $[Fe^{2+}]/[Fe^{3+}]$ in the right half-cell. The Pt wire is the indicator electrode, and the entire left half-cell plus salt bridge (enclosed by the dash line) can be considered to be a reference electrode.**

Reference Electrode: Ag/AgCl

- **Reference Electrode : Ag | AgCl | Cl^- + Salt Bridge**

  → Constant potential

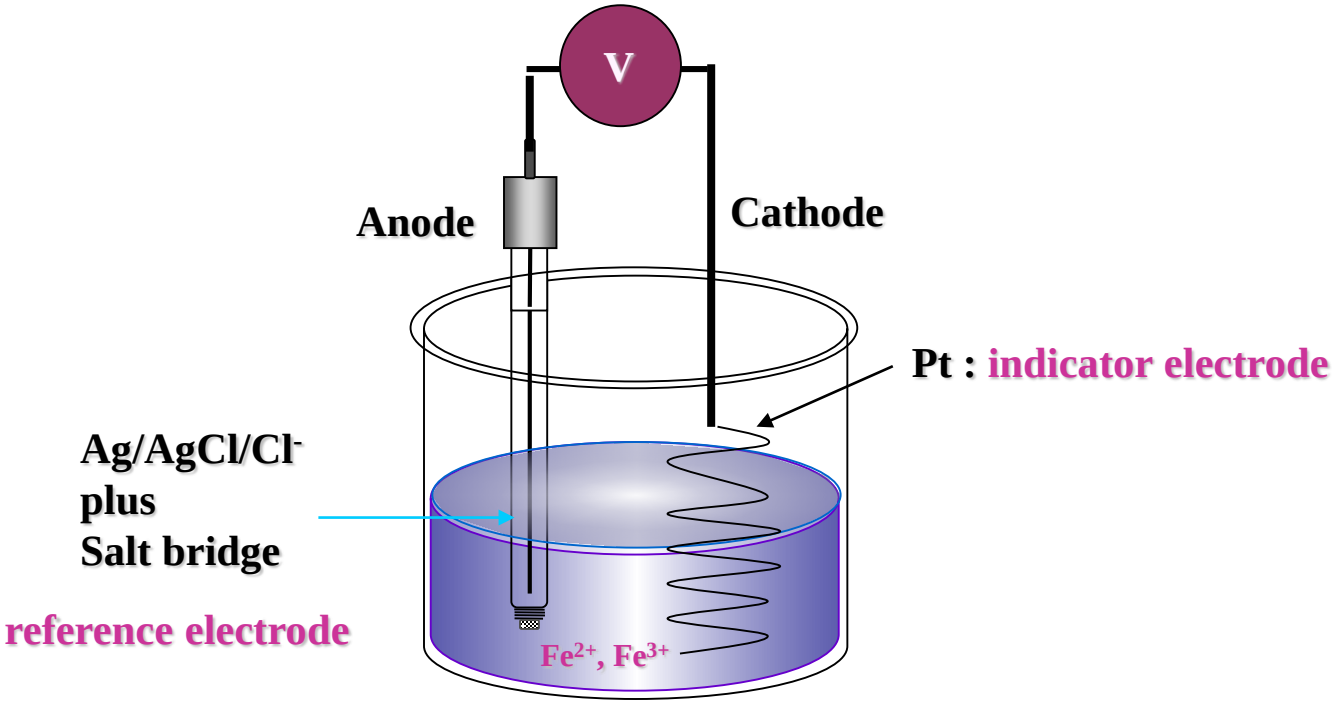

- **Fig. Another view of Figure 15.1. The contents of the colored box in Figure 15.1 are now considered to be a reference electrode dipped into the analyte solution.**

Ion Selective Electrode (ISE)

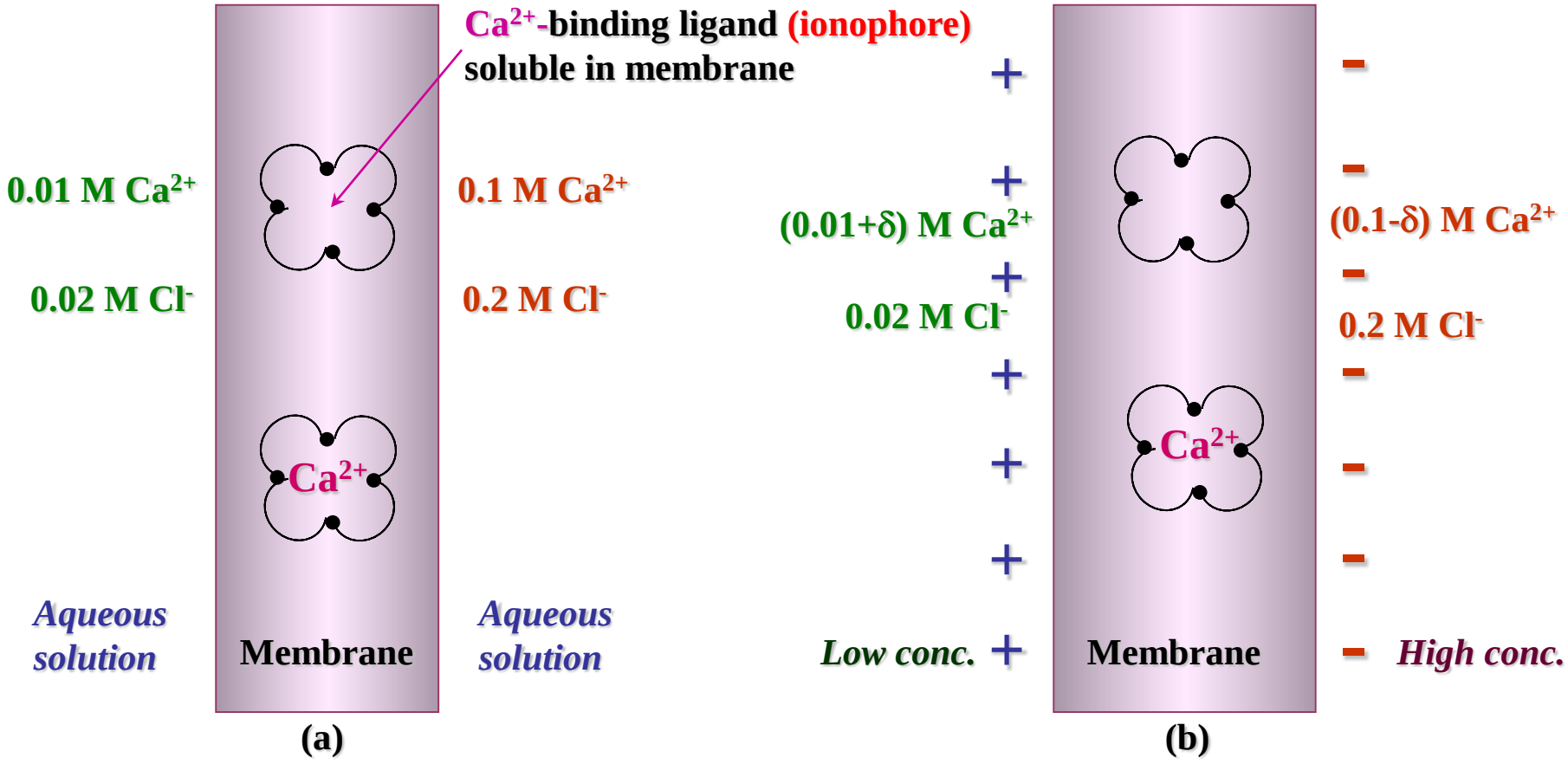

- **Fig.** Mechanism of ion-selective electrode. (a) Initial conditions prior to Ca^{2+} migration across the membrane. (b) After δ moles of Ca^{2+} per liter have crossed the membrane, giving the left side a charge of $+2\delta$ mol/L and the right side a charge of -2δ mol/L.

Ion Selective Electrode (ISE)

Concentration difference → free energy difference : membrane potential

$$\Delta G = -RT \ln \frac{A1}{A2}$$

$$\Delta G = -nFE$$

$$-RT \ln \frac{A1}{A2} = -nFE$$

$$E_{memb} = RT/nF \ln \frac{A1}{A2} = \frac{0.05916}{n} \log \frac{A1}{A2} \text{(volts at 25℃)}$$

E_{memb}: membrane potential

1: Sample solution, 2: Internal solution

$Ca^{2+} \rightarrow n = 2$

10-fold change in $[Ca^{2+}] \rightarrow 59.16/2 = 29.58$ mV change

Ion Selective Electrode (ISE)

$$E_{cell} = E_{ref\cdot ext} - E_{ref\cdot int} + E_{memb} + E_{lj}$$

$$E_{cell} = E_{ref\cdot ext} - E_{ref\cdot int} + \frac{RT}{ZF} \ln \frac{1}{(a_i)int} + E_{lj} + \frac{RT}{ZF} \ln (a_i)\ \text{sample}$$

Constant

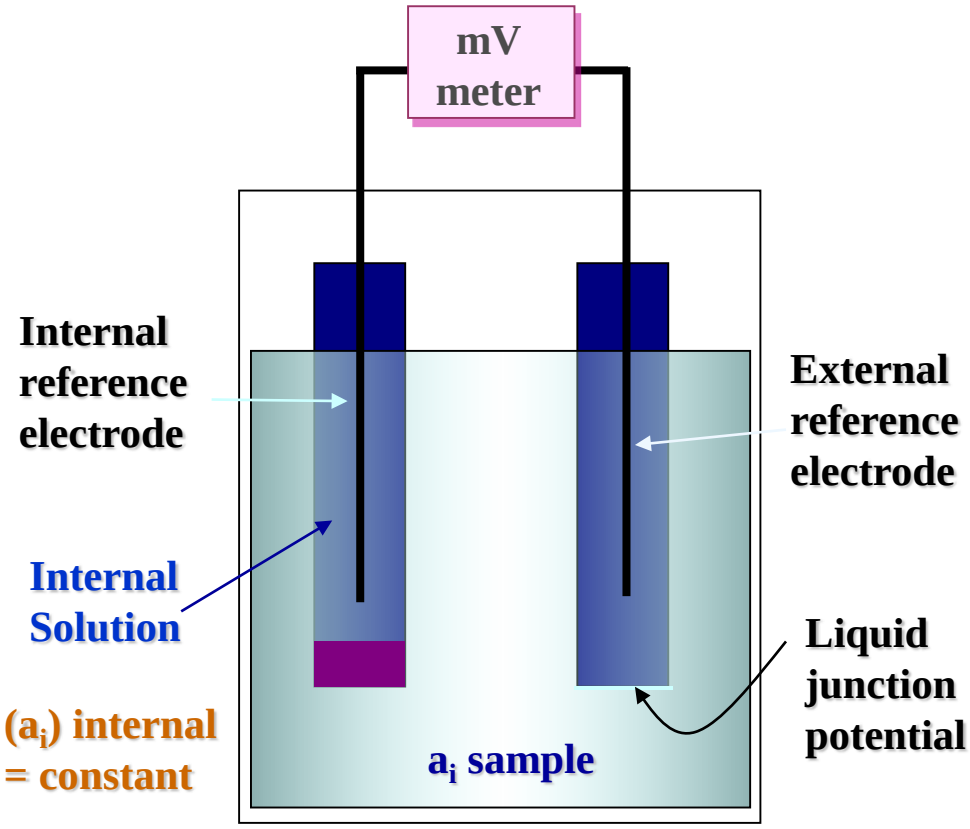

$$E_{cell} = K + \frac{RT}{ZF} \ln (a_i)\ \text{sample}$$

$$E_{cell} = K + \frac{0.05916}{n} \log (a_i)\ \text{sample}$$

(n = Z) *at 25 ℃*

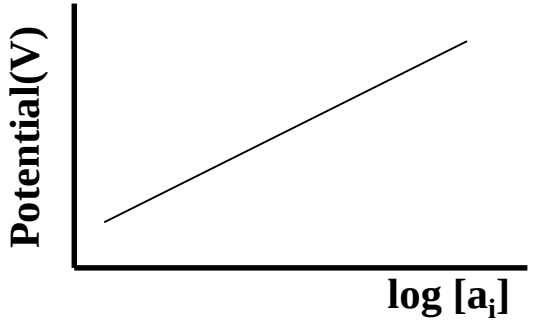

Selectivity Coefficients in ISE

- Since membrains respond to a certain degree to ions other than the analyte (i.e. interferents)
- **A more general expression:**

$$E_{cell} = k + \frac{RT}{ZF} \ln(a_i + k_{ij} a_j^{z/x})$$

a_i = activity of analyte ion. i

a_j = activity of interferent ion. j

x = charge of interferent ion

k_{ij} = selectivity constant

k_{ij} = response to j/response to i

For Na^+, K^+ = 1/2800

- **Small values of k_{ij} are characteristics of electrode with good selectivity for the analyte, *i***

Ionophores (neutral carriers) for ISE

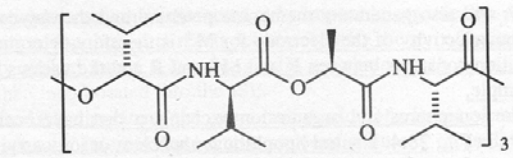

antibiotic

Valinomycin

K^+

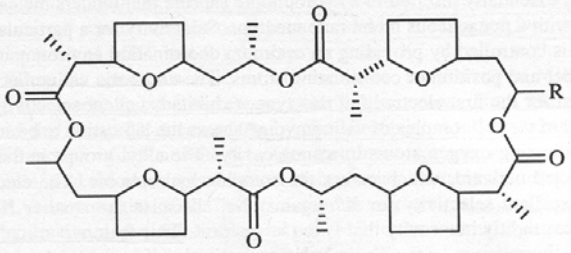

R = CH_3: nonactin

R = C_2H_5: monactin

NH_4^+

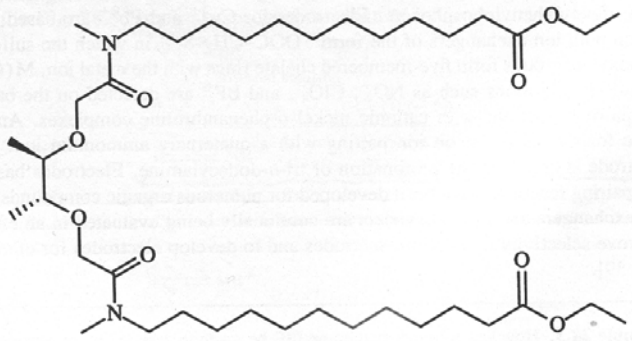

ETH 1001

Ca^{2+}

Fig. 28.4 Ionophores (20) and ion exchangers for liquid and polymer membrane ISEs.

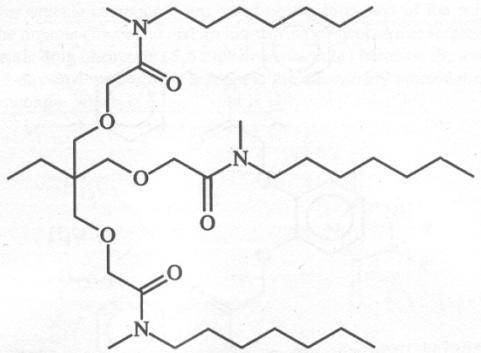

ETH 227

Na^+ ($Na^+ > K^+$)

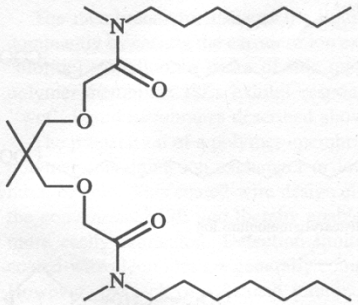

ETH 149

Li^+

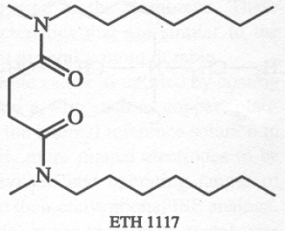

ETH 1117

Mg^{2+}

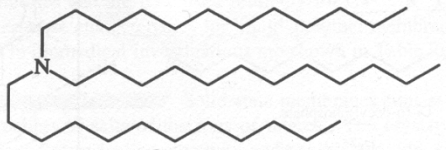

Tri-*n*-dodecylamine

H^+

Fig. 28.4 (*Continued*)

Ionophores (neutral carriers) for ISE

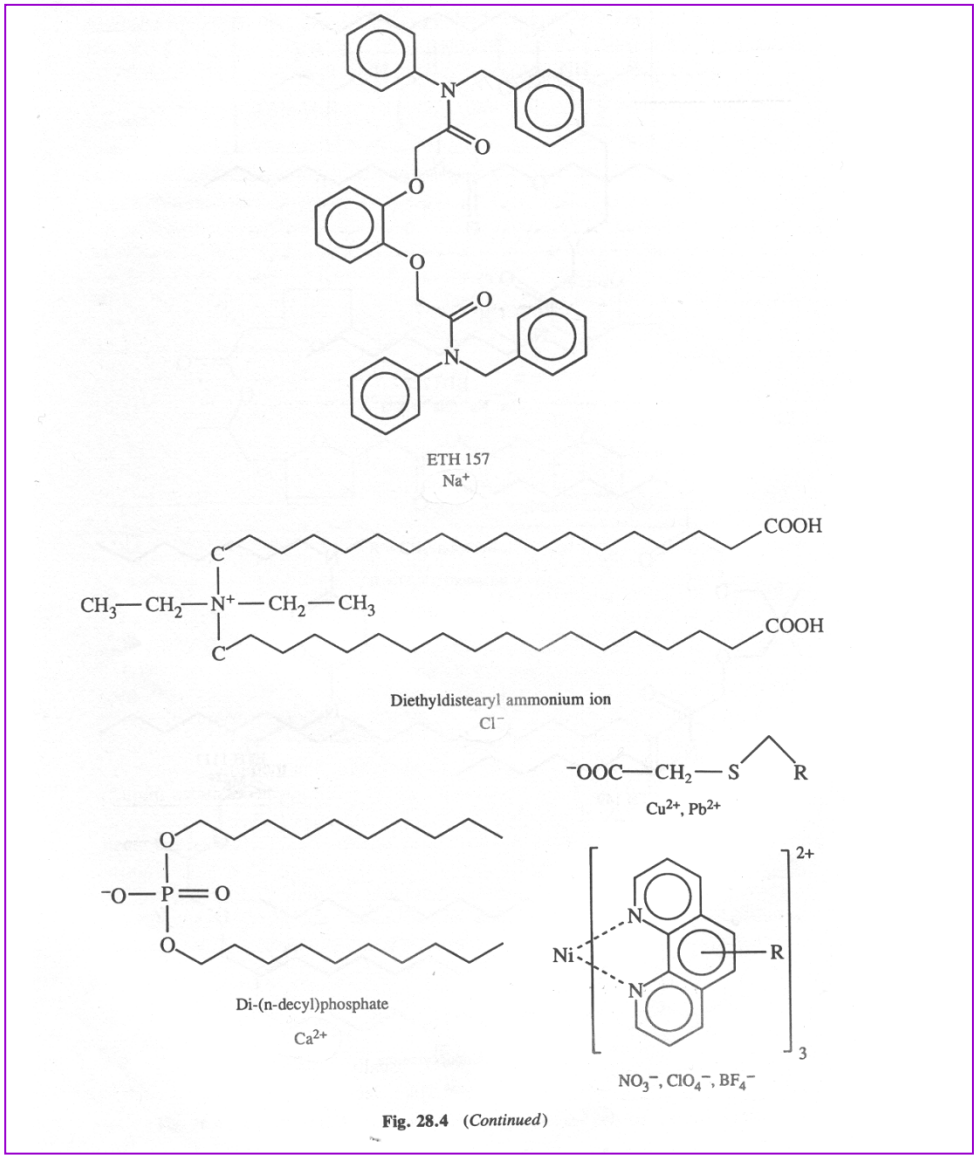

Fig. 28.4 (*Continued*)

Selectivity of Li – ion selective electrode

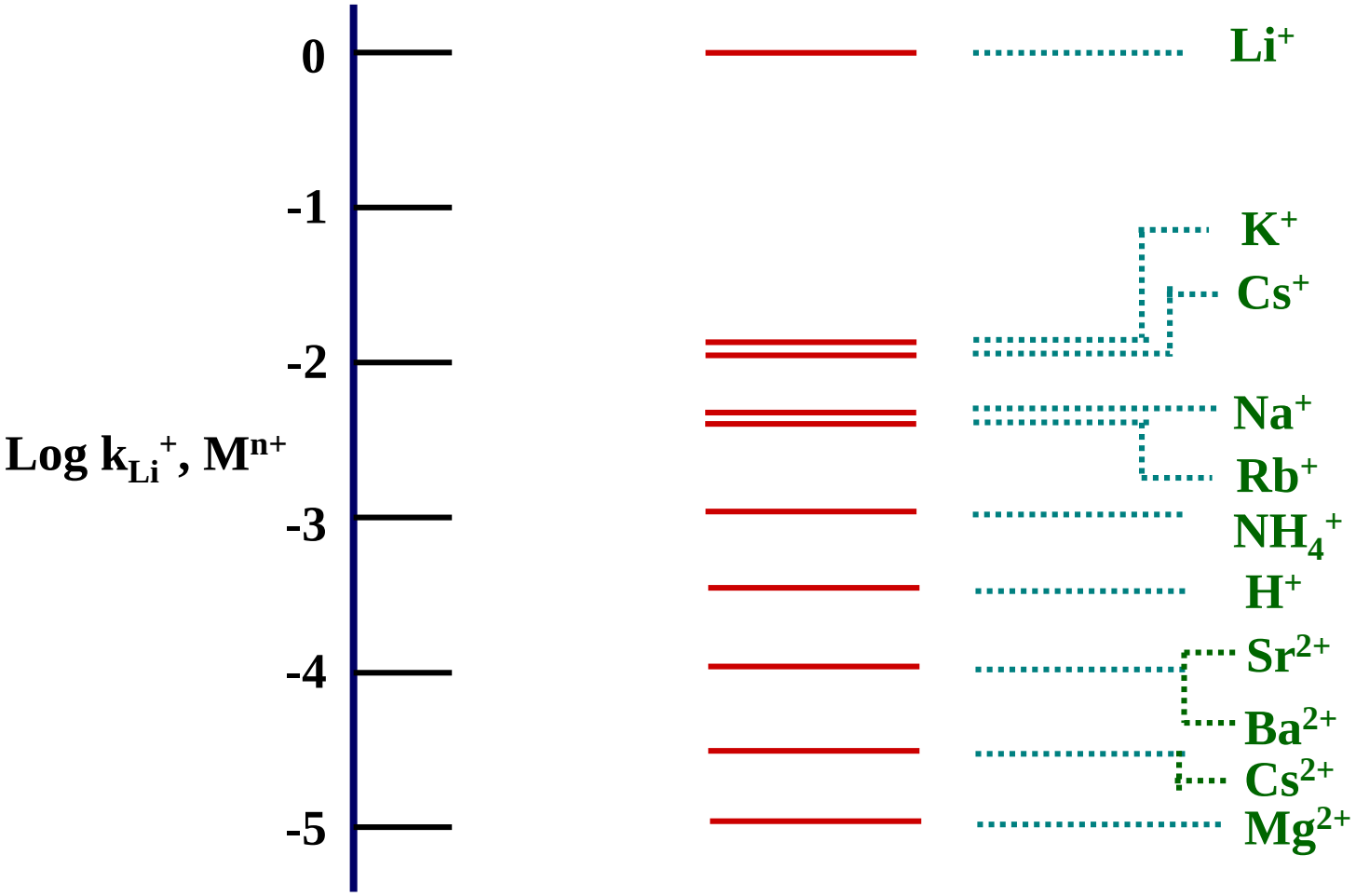

Anal. Chem. **2000,** *72,* 2200−2205

Design and Synthesis of a More Highly Selective Ammonium Ionophore Than Nonactin and Its Application as an Ion-Sensing Component for an Ion-Selective Electrode

Koji Suzuki,*,†,‡ Dwi Siswanta,† Takeshi Otsuka,† Tsuyoshi Amano,† Takafumi Ikeda,† Hideaki Hisamoto,†,|| Ryoko Yoshihara,§ and Shigeru Ohba§

Department of Applied Chemistry and Department of Chemistry, Keio University, 3-14-1 Hiyoshi, Kohoku-ku, Yokohama 223-8522, Japan, and Kanagawa Academy of Science and Technology (KAST), KSP West-614, 3-2-1 Sakato, Kawasaki 213-0012, Japan

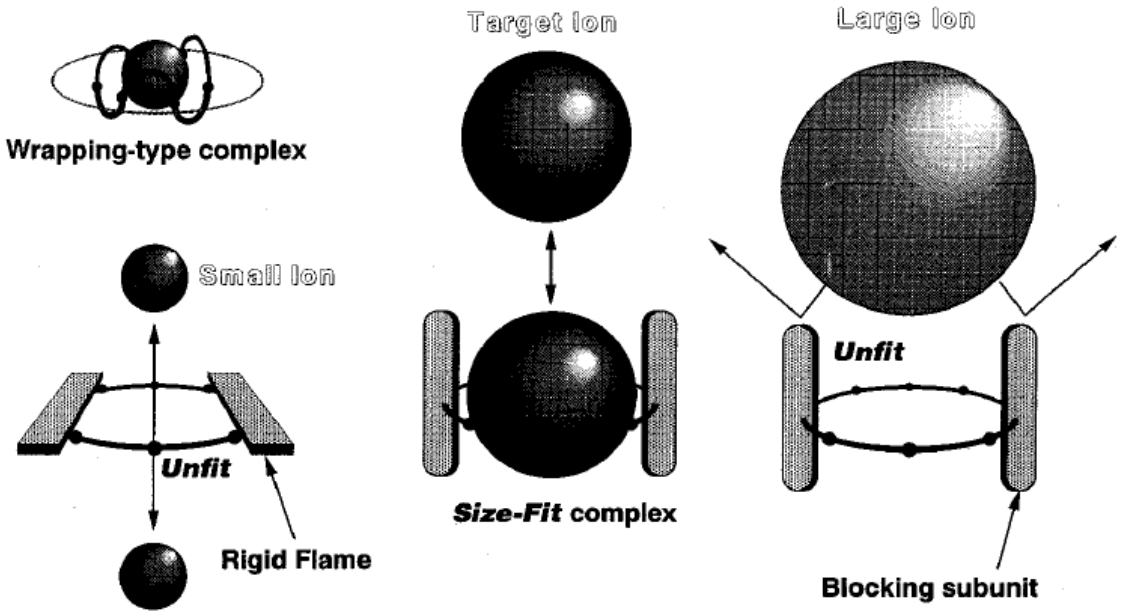

Figure 1. Effective molecular structure design for ammonium ionophore (target ion, NH_4^+).

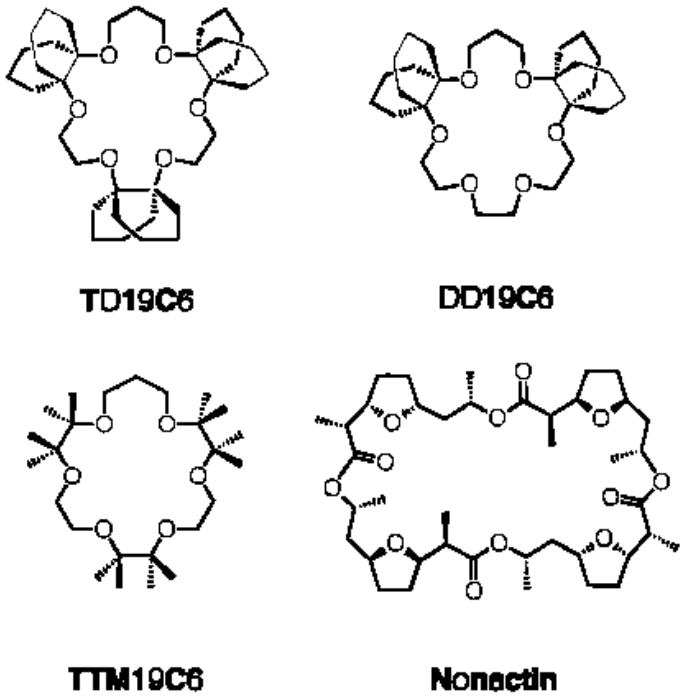

Figure 2. Chemical structures of the newly synthesized ammonium ionophores (TD19C6, DD19C6, TTM19C6) which have a 19-membered-crown ring with three or two bulky block subunits and nonactin.

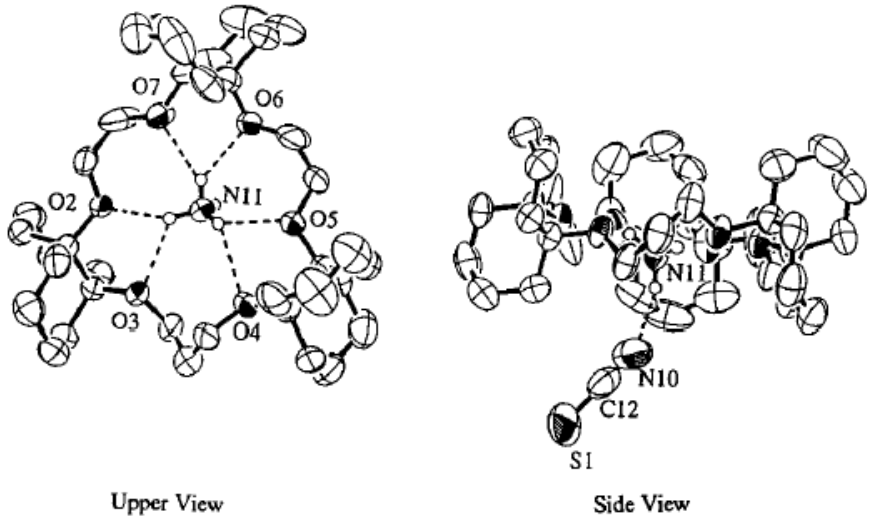

Figure 4. Steric chemical structures of TD19C6–NH_4^+ complex determined by X-ray analysis.

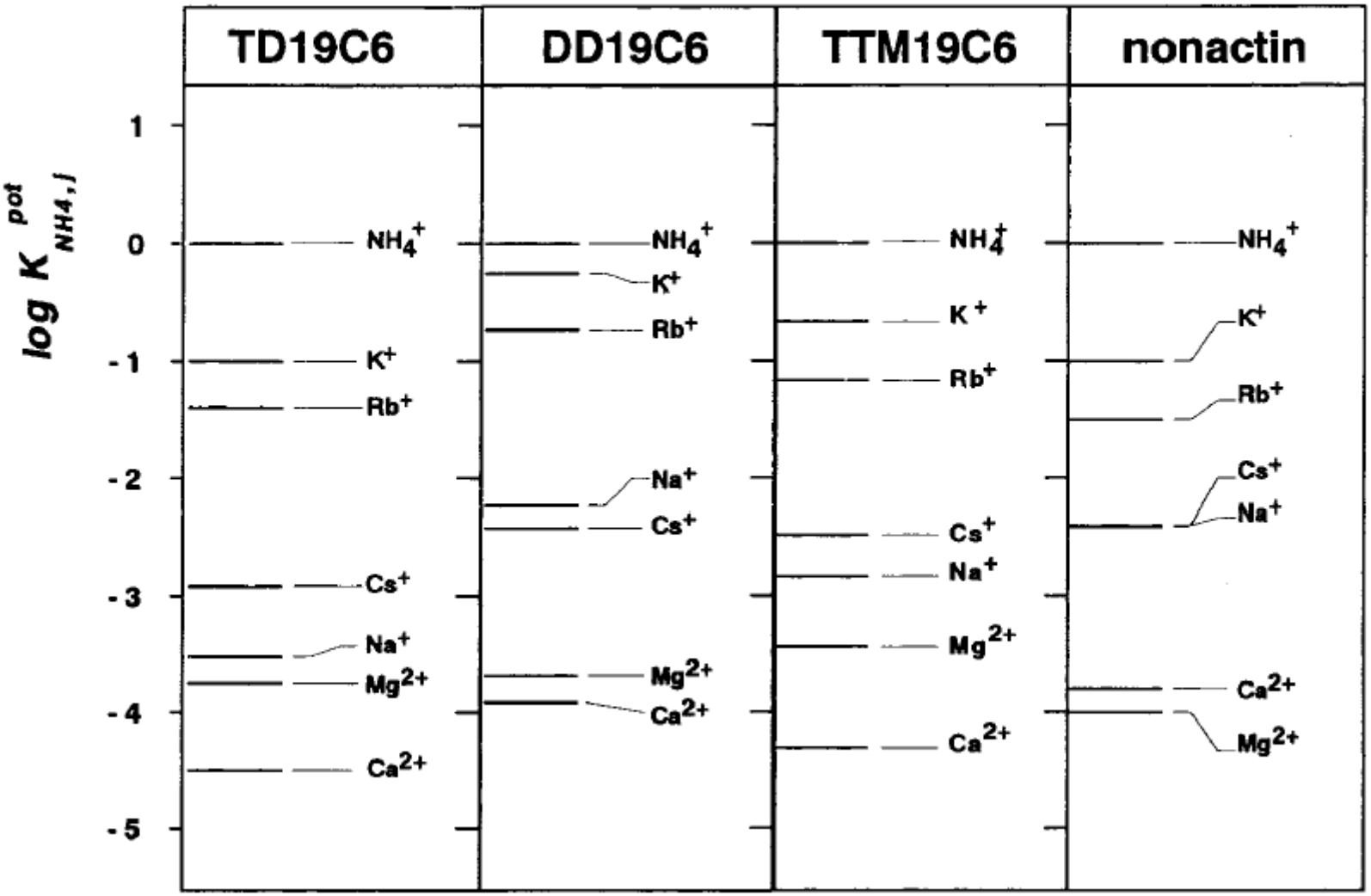

Figure 3. Selectivity coefficients of the ammonium ion-selective electrodes based on TD19C6, DD19C6, TTM19C6, and nonactin. The membrane compositions for the three ionophores based on 19C6 derivatives were 3 wt % ionophore, 10 mol % (of the ionophore content) KTCPB, 67 wt % BBPA, and ~30 wt % PVC. The ion-selectivity factors of the nonactin-based electrode were obtained from ref 9.

pH Electrode (Glass-membrane electrode)

- Glasses of certain compositions respond to pH due to a membrane potential generated by an ion-exchange mechanism with H^+

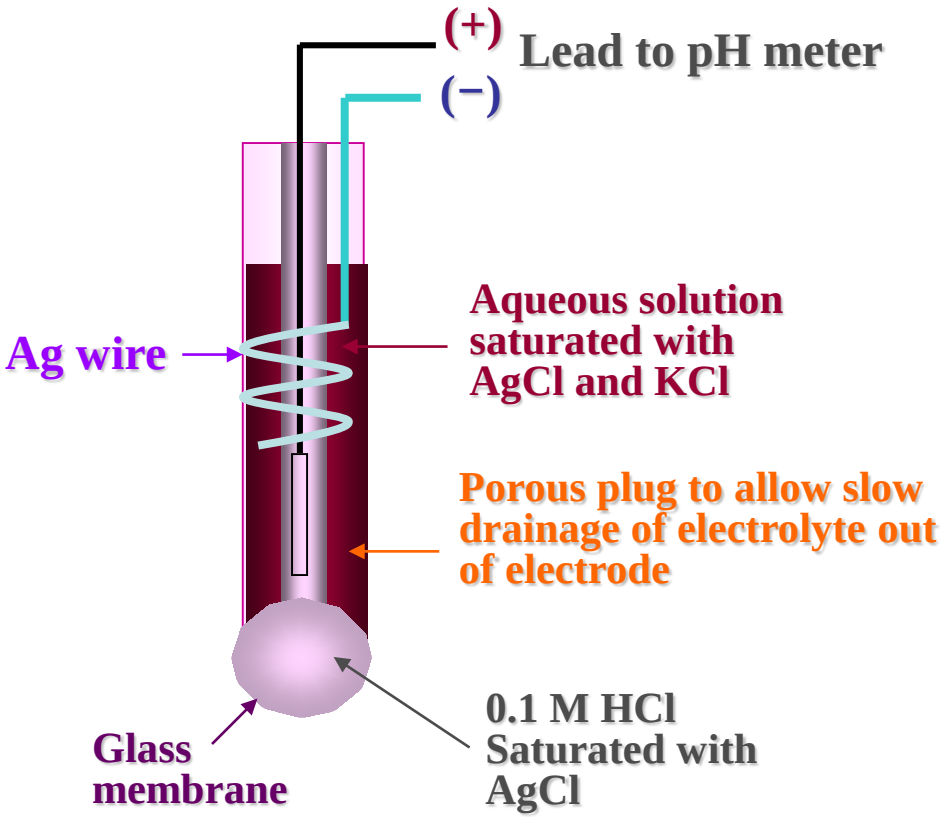

- Fig. 15.9 Diagram of a glass combination electrode having a silver-silver chloride reference electrode. The glass electrode is immersed in a solution of unknown pH so that the porous plug on the lower right is below the surface of the liquid. The two silver electrodes measure the voltage across the glass membrane.

Glass : 22% Na_2O, 6% CaO, and 72% SiO_2 (Corning 015 glass membrane)

Gas-Sensing Electrode : (compound electrode)

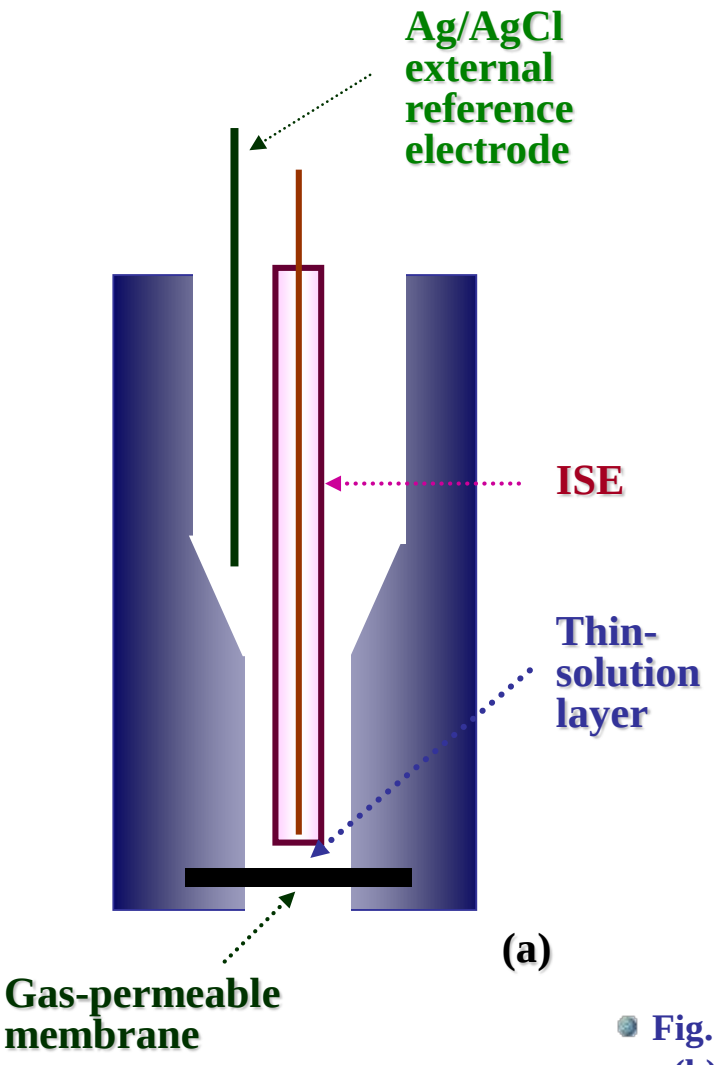

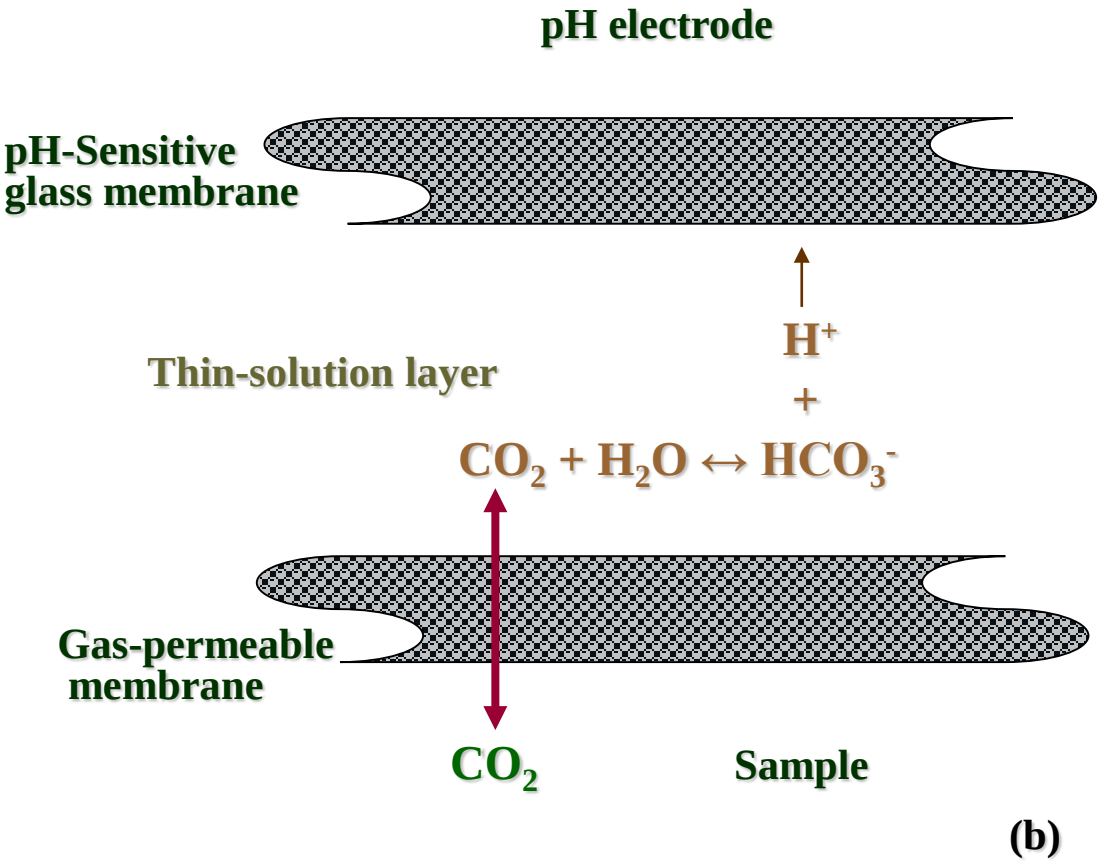

Fig. 28.8 Schematic representation of (a) gas-sensing electrode and (b) membrane and thin layer of electrolyte region of CO_2 electrode.

Gas-Sensing Electrode : (compound electrode)

- **Table 28.3 Gas-Sensing Electrodes**

Gas Electrode	Internal Solution Equilibrium	Sensing Element
CO_2	$CO_2 + H_2O \leftrightarrow HCO_3 + H^+$	Glass, pH
NH_3	$NH_3 + H_2O \leftrightarrow NH_4^+ + OH^-$	Glass, pH
HCN	$HCN \leftrightarrow H^+ + CN^-$	Ag_2S, pCN
HF	$HF \leftrightarrow H^+ + F^-$	LaF_3, pF
H_2S	$H_2S \leftrightarrow 2H^+ + S^{2-}$	Ag_2S, pS
SO_2	$SO_2 + H_2O \leftrightarrow HSO_3^- + H^+$	Glass, pH

Bio-catalytic Membrane Electrode (potentiometric biosensor)

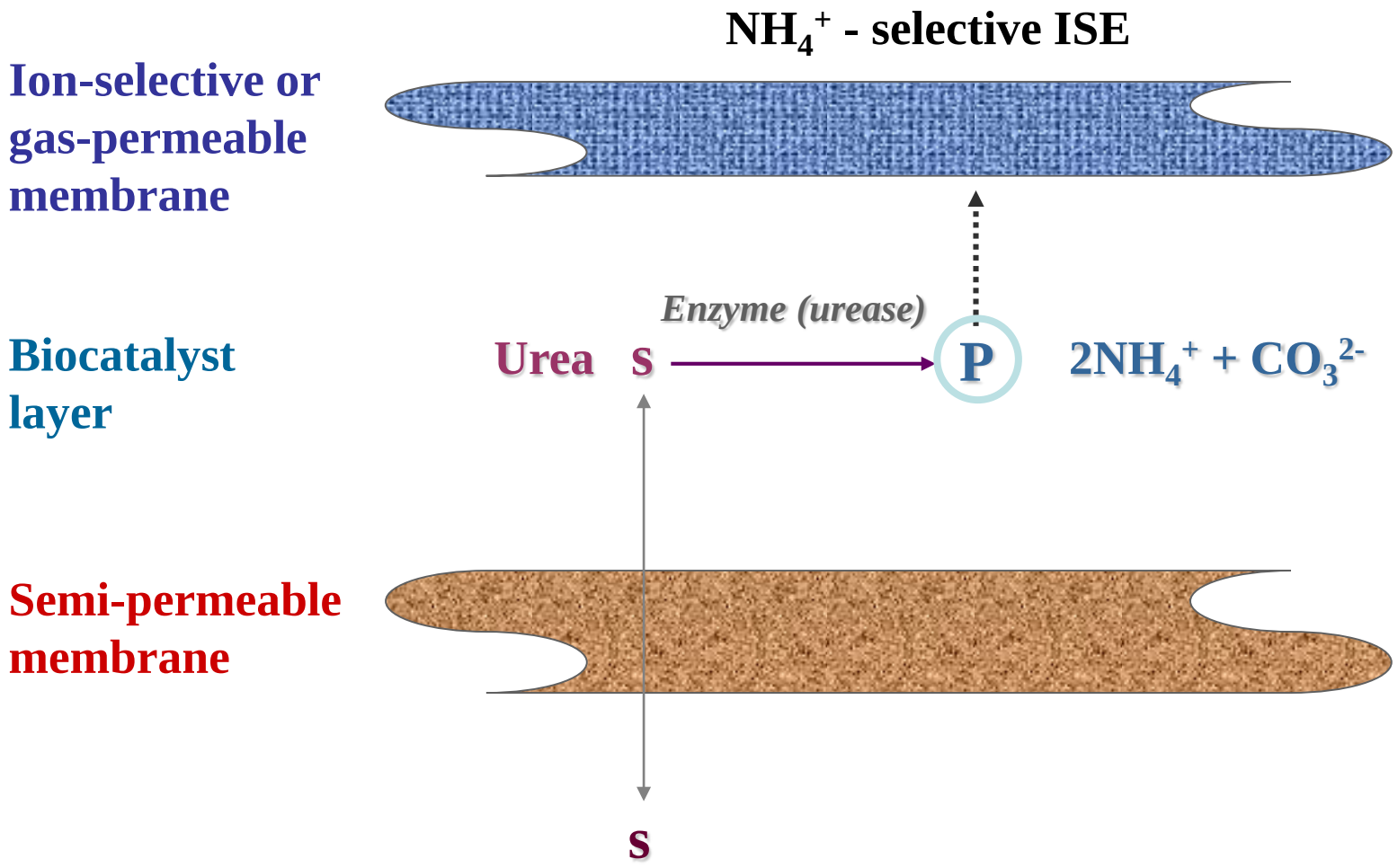

Fig. 28.9 Schematic diagram of biocatalytic electrode.

Bio-catalytic Membrane Electrode (potentiometric biosensor)

- **Table 28.4 Representative Biocatalytic Membrane Electrode**

Biocatalyst Category	*Substrate*	*Biocatalyst*	*Detected Substance*
Enzyme	Urea	Urease	NH_4^+, NH_3,CO_2, or H^+
	Glucose	Glucose oxidase and peroxidase	I^-
		Glucose oxidase	H^+
		Glucose oxidase	F^-
	Amygdalin	β-glucosidase	CN^-
	Pencillin	Penicillinase	H^+
	L-phenylalanine	L-amino acid oxidase	NH_4^+
		L-amino acid oxidase and horseradish peroxidase	I^-
		Phenylalanine ammonia lyase	NH_3
		Phenylalanine decarboxylase	CO_2
	Uric acid	Uricase	CO_2
	Acetylcholine	Acetylcholinesterase	H^+
	D-gluconate	Gluconate kinase and 6-phospho-D-gluconate dehydrogenase	CO_2
	Acetaldehyde	Aldehyde dehydrogenase	H^+
	Oxalate	Oxalate decarboxylase	CO_2
	Flavin adenine dinucleotide	Alkaline phosphatase and adenosine deaminase	NH_3
	Methotrexate	Dihydrofolate reductase and 6-phosphogluconic dehydrogenase	CO_2
	Salicylate	Salicylate hyroxylase	CO_2
Bacterial particle	L-arginine	*Streptococcus faecium*	NH_3
		Streptococcus lactis	NH_3
	L-aspartate	*Bacterium cadaveris*	NH_3
	L-glutamine	*Sarcina flava*	NH_3
	NAD^+	*Escherichia coli*/NADase	NH_3
	Nitrilotriacetate acid	*Pseudomonas* sp.	NH_3
	L-tyrosine	*Aeromonas phenologenes*	NH_3
	L-histidine	*Pseudomonas* sp.	NH_3
	L-serine	*Clostridium acidiurici*	NH_3
	Nitrate	*Azotobacter vinelandii*	NH_3
	Uric acid	*Pichia membranaefaciens*	CO_2
	L-glutamic acid	*Escherichia coli*	CO_2
Bacterial particle	Pyruvate	*Streptococcus faecium*	CO_2
	L-cysteine	*Proteus morganii*	H_2S
	Sugars	Bacteria from human dental plaque	H^+
Tissue	Glucosamine 6-phosphate	Porcine kidney tissue	NH_3
	L-cysteine	Treated plant leaf	
	Adenosine	Mouse small intestine mucosal cells	NH_3
	Adenosine 5′-monophosphate	Rabbit muscle	NH_3
	L-glutamate	Yellow squash	CO_2
	Glutamine	Porcine kidney cortex	NH_3
	Guanine	Rabbit liver	NH_3

Microfluidic and Biosensor Chip Technology (Multibiosensor)

Sodium, Potassium, Chloride, Ionized Calcium, pH and PCO_2 by ion-selective electrode potentiometry.

Urea is first hydrolyzed to ammonium ions in a reaction catalyzed by the enzyme urease. The ammonium ions are measured by an ion-selective electrode.

Glucose is measured amperometrically.

PO_2 is measured amperometrically.

Hematocrit is determined conductometrically.

HCO_3, TCO_2 , BE, sO_2, Anion Gap and Hemoglobin.

"Chem 7" test:

Na+, K^+, Cl^-, total CO_2,

glucose, urea, creatinine

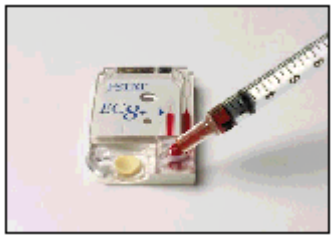

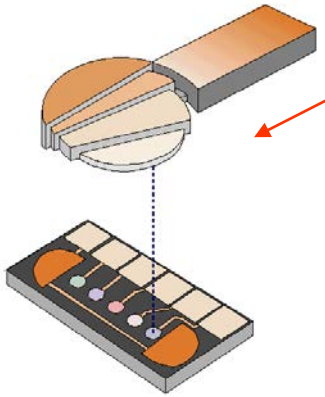

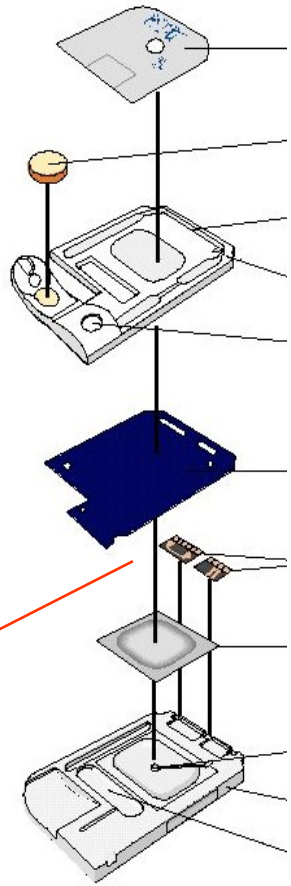

Voltammetry

Control of cell voltages

Measurement of current

Electrochemical cells

Microelectrodes for working electrodes

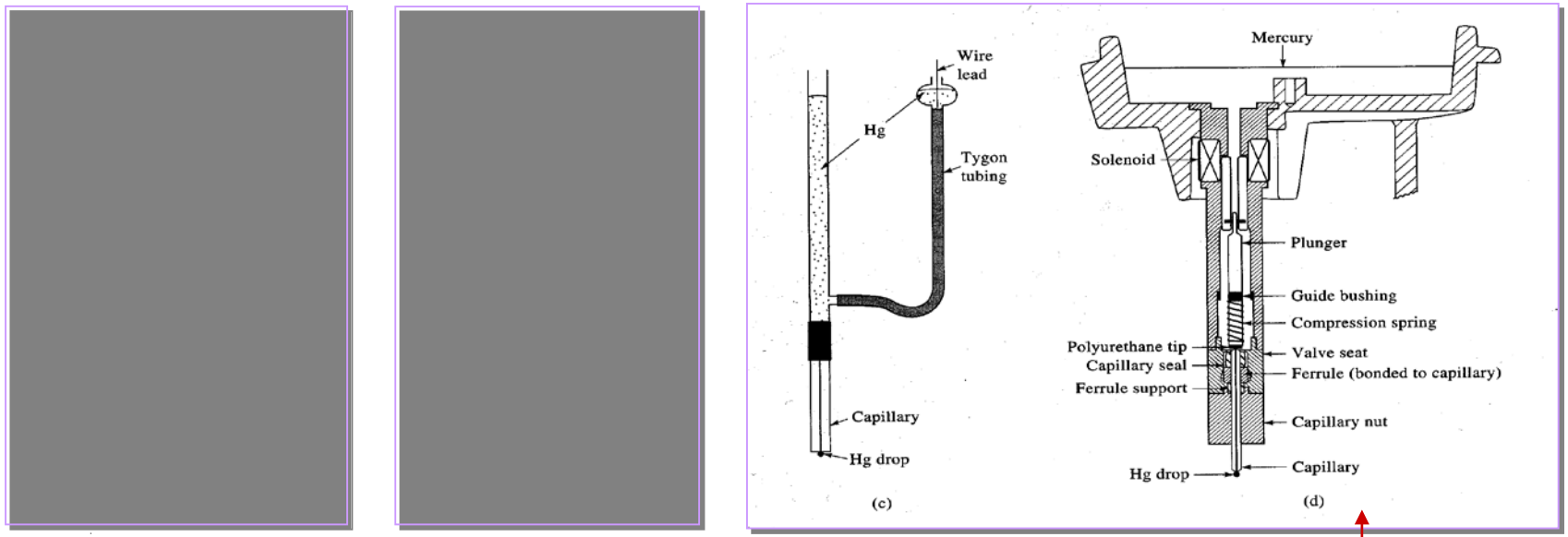

Figure 25-3 Some common types of microelectrodes: (a) a disk electrode, (b) a hanging mercury drop electrode, (c) a dropping mercury electrode, (d) a static mercury drop electrode.

- drop diameter : 0.1 ~ 1.0 mm
- A new drop forms and breaks every 2 ~ 6 s

- commercially available: can be operated as a dropping mercury electrode or hanging mercury drop electrode

Commercial Potentiostats

Potentiostat vs Galvanostat

- A potentiostat is used to apply a controlled potential to an electrochemical cell and measured the current response.
- A galvanostat is used to apply a controlled current.

EG&G PAR 273A

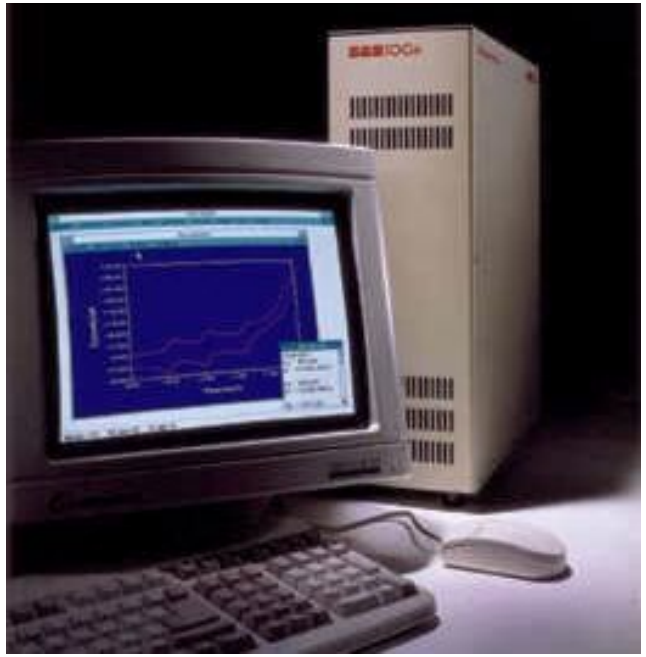

BAS 100B/W

Electrochemical Cells for Voltammetric Sensors

Control E – measure i

voltammetry – scan E

amperometry – hold E

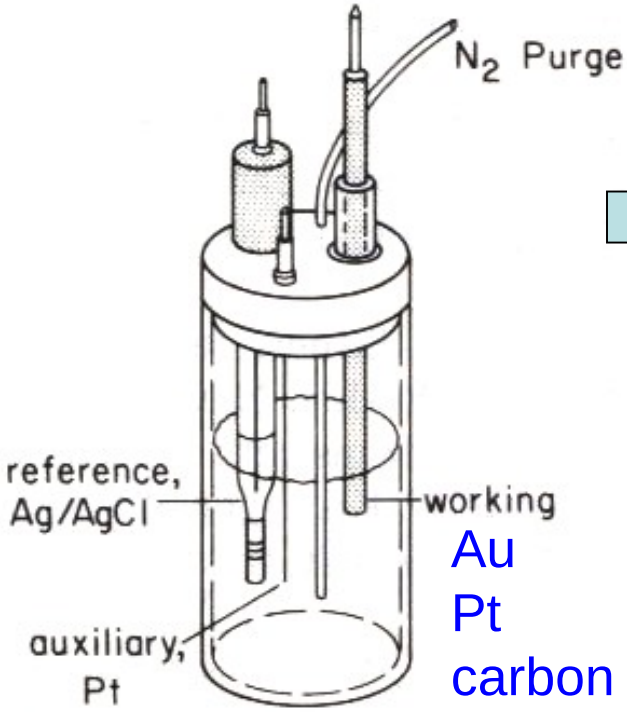

Au

Pt

carbon

3 electrode

BAS, Inc.

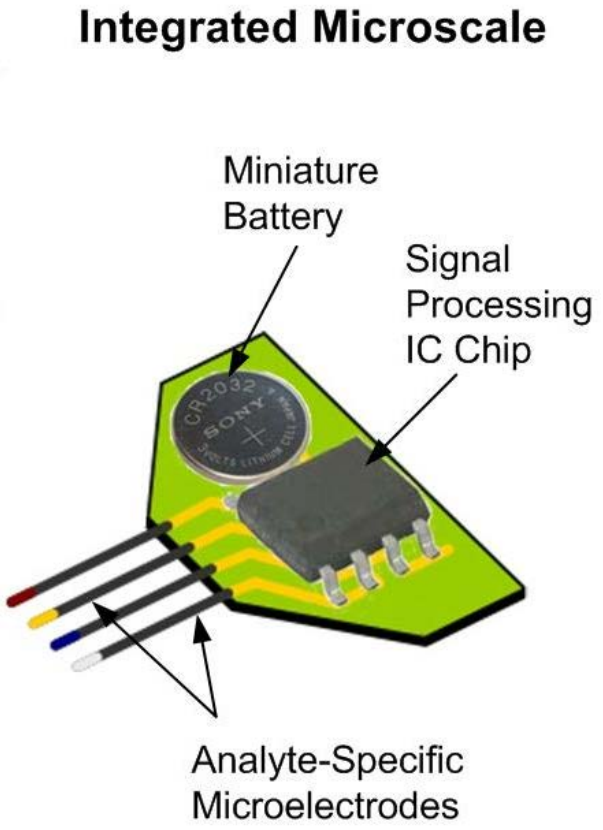

Adapted from Sawyer, Heineman & Beebe,
Chemistry Experiments for Instrumental Methods, Wiley

Biosensor Design

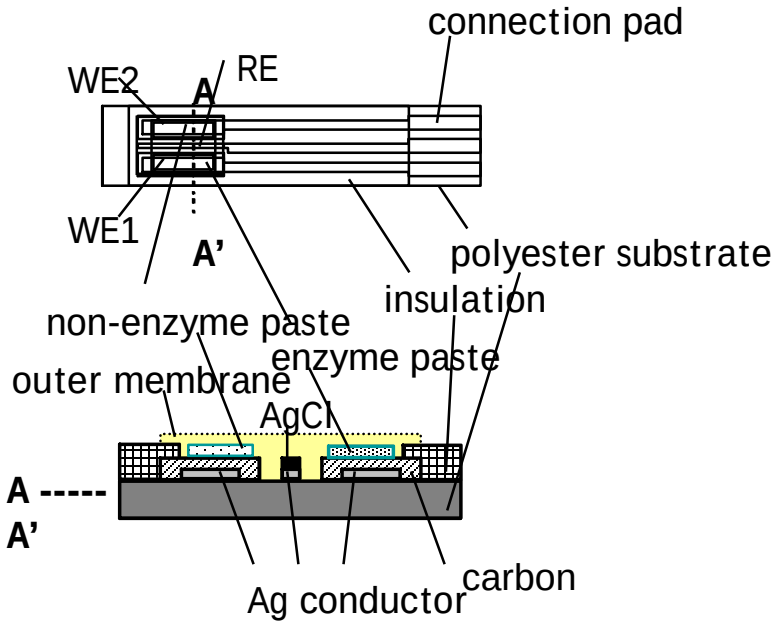

Fabrication Process

Screen printing technology for thick-film electrode

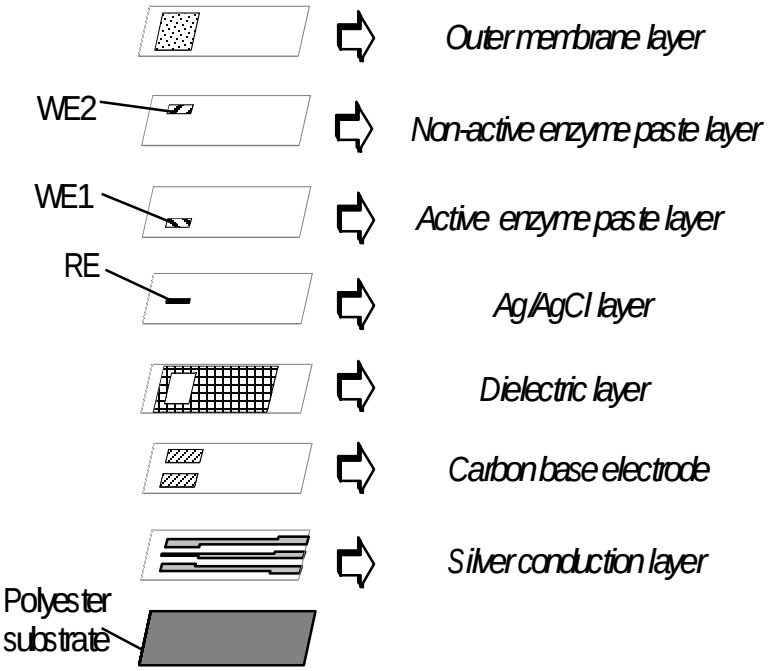

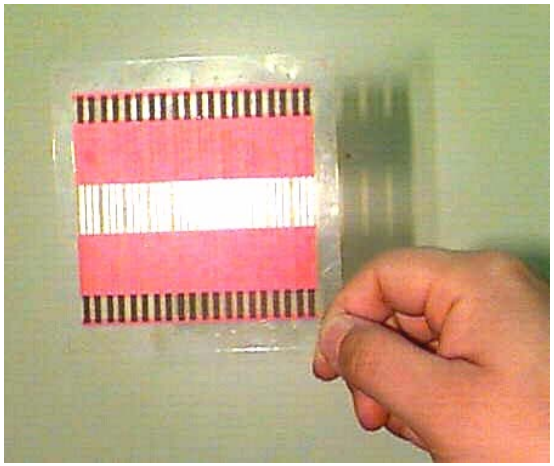

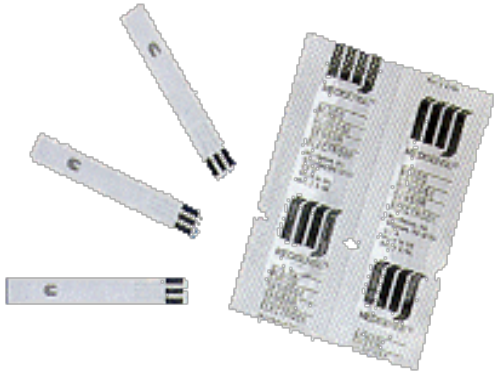

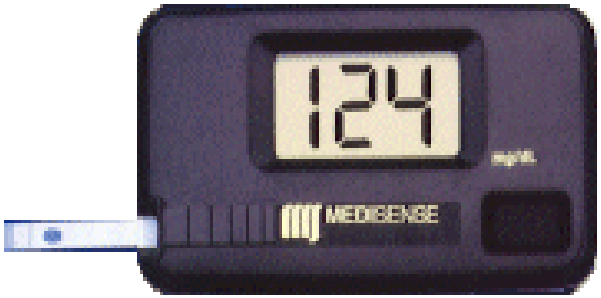

Electrochemical cells

Reference electrode (ideal non-polarized electrode)

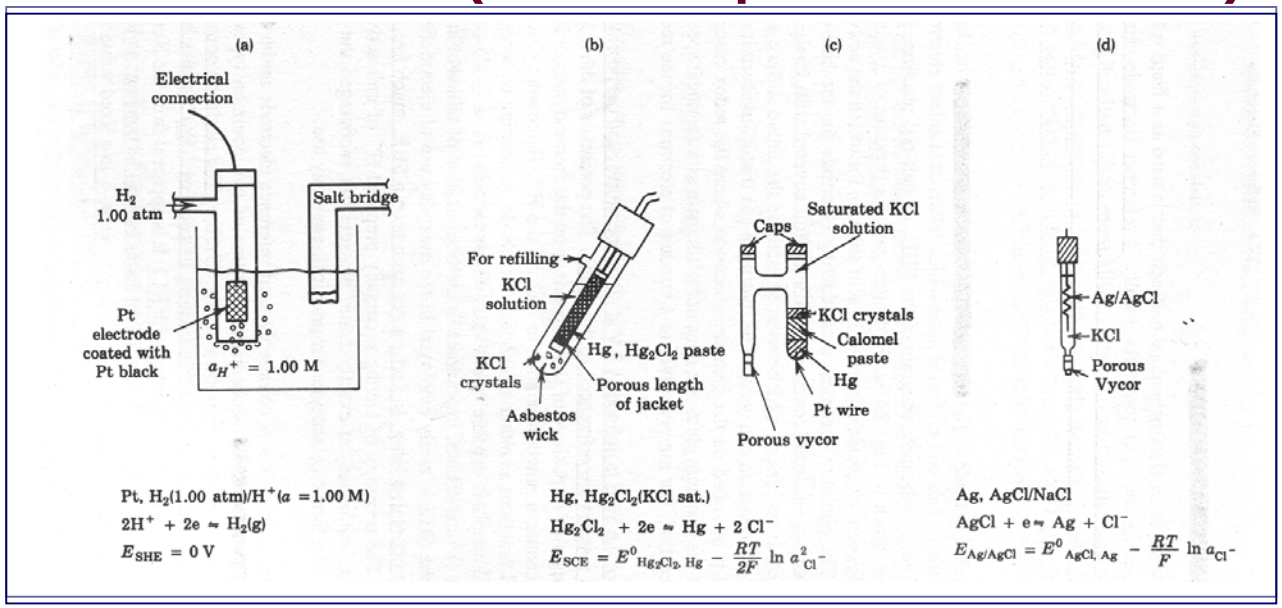

- E - I curves for reference and working electrode
  - reference electrode

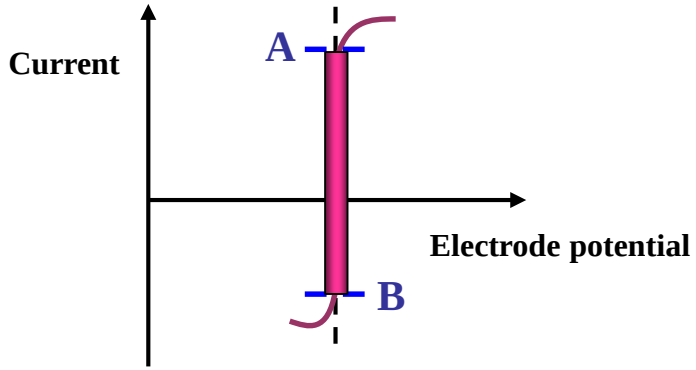

  - working electrode (ideal polarizable electrode)

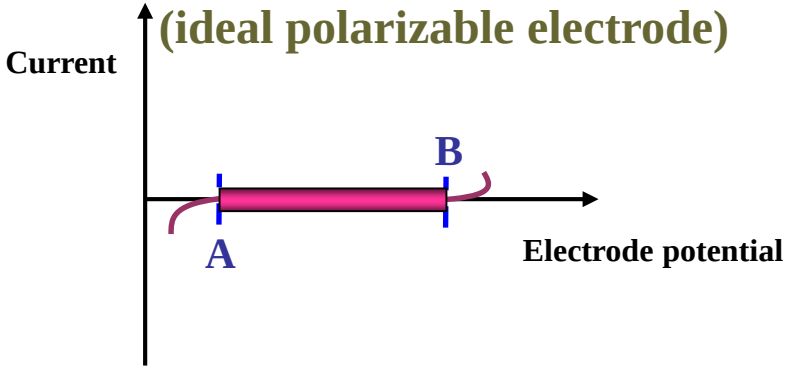

Schematic diagram of the electrochemical cell

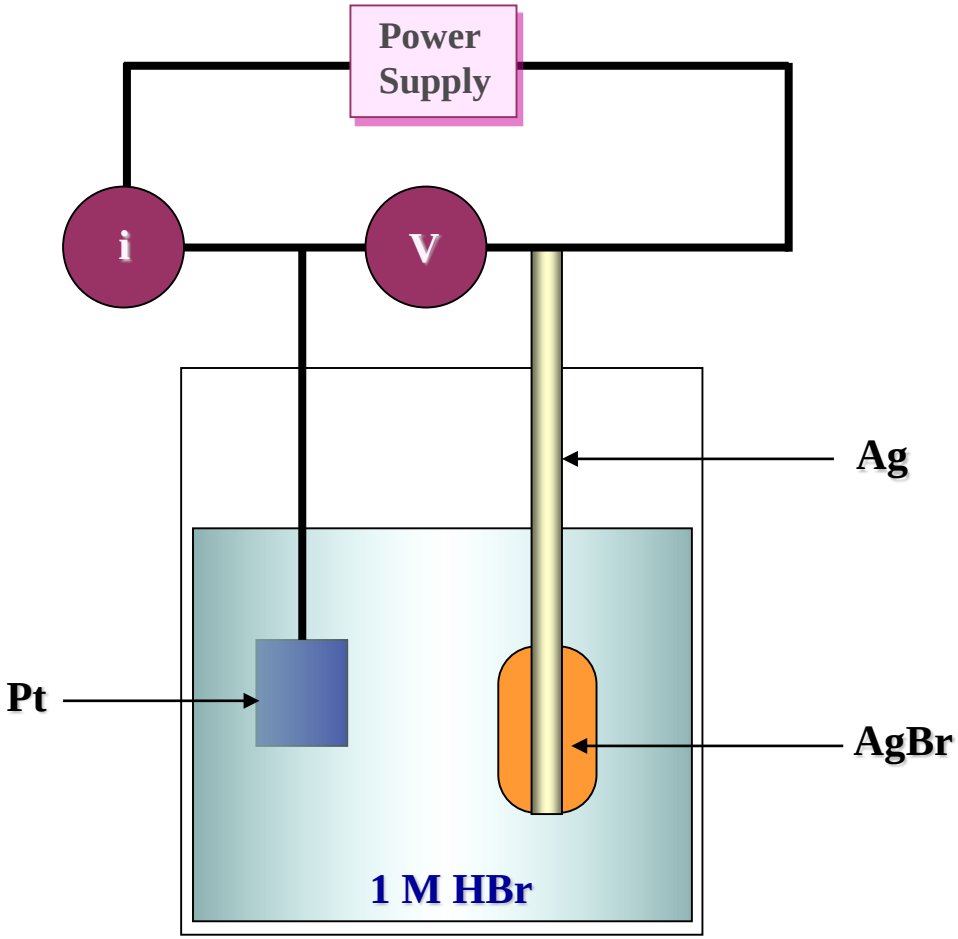

Reference electrode

$$AgBr + e \rightleftharpoons Ag + Br^-$$

$$(E^0 = 0.0713\ V\ vs\ NHE)$$

Fig. 1.1.3 Schematic diagram of the electrochemical cell Pt/HBr(1 M)/AgBr/Ag attached to power supply and meters for obtaining a current-potential(i-E) curve.

Schematic Current-Potential Curve

Use of Pt electrode

Negative direction scan

- H^+ reduction at Pt electrode

$$2H^+ + 2e \rightarrow H_2$$

(E^0 = 0 V vs NHE or -0.07 V vs Ag/AgBr)

- Oxidation at reference electrode

$$Ag + Br^- \rightarrow Ag^+Br^- + e^-$$

(Br^- concentration no change→ no potential change)

Positive direction scan

- Br^- oxidation at Pt electrode

$$2Br^- \rightarrow Br_2 + 2e^-$$

(E^0 = +1.09 V vs NHE or +1.02 V vs Ag/AgBr)

Reduction at reference electrode

$$Ag^+Br^- + e^- \rightarrow Ag + Br^-$$

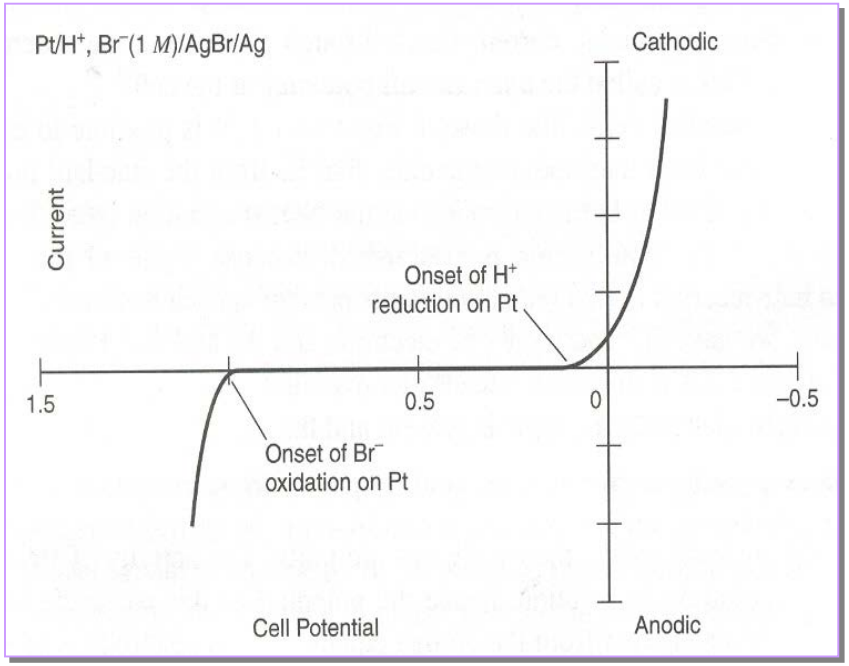

Fig. 1.1.4 Schematic current-potential curve for the cell Pt/K^+, Br^- (1 M)/AgBr/Ag, showing the limiting proton reduction and bromide oxidation processes. The cell potential is given for the Pt electrode with respect to the Ag electrode, so it is equivalent to E_{pt}(V vs AgBr). Since $E_{Ag/AgBr}$ = 0.07 V vs NHE, the potential axis could be converted to E_{pt}(V vs NHE) by adding 0.07 V to each value of potential.

Schematic Current-Potential Curve

Use of Hg electrode

Negative direction scan

- The heterogeneous rate constant for H_2 evolution at Hg electrode is much lower than at Pt.
- The heterogeneous rate constant is a function of applied potential.
- The additional potential (beyond the thermo-dynamic requirement) needed to drive a reaction at a certain rate is called

overpotential : $\eta = E_{app} - E_{eq}$

Positive direction scan

- Mercury oxidation

$$Hg_2Br_2 + 2e \rightarrow 2Hg + 2Br^-$$

(E^0 = +0.14 V vs NHE or +0.07 V vs Ag/AgBr)

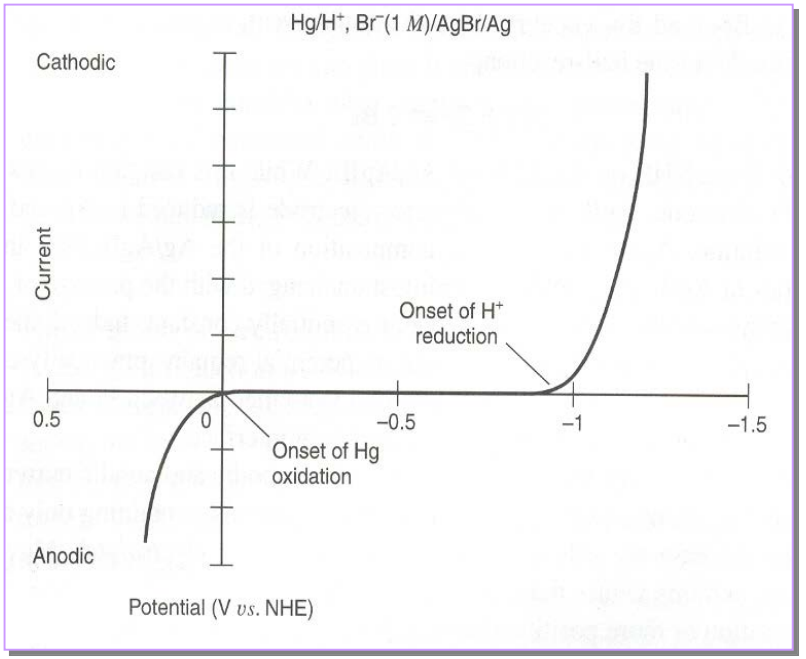

Fig. 1.1.5 Schematic current-potential curve for the Hg electrode in the cell $Hg/H^+, Br^-(1\ M)/AgBr/Ag$, showing the limiting process : proton reduction with a large overpotential and mercury oxidation. The potential axis is defined through the process outlined in the caption to Figure 1.1.4

Overpotential

$$H_3O^+ + e^- \rightarrow \tfrac{1}{2} H_2 + H_2O$$

The reaction begins -0.35 V at Pt -0.8 V at Ag

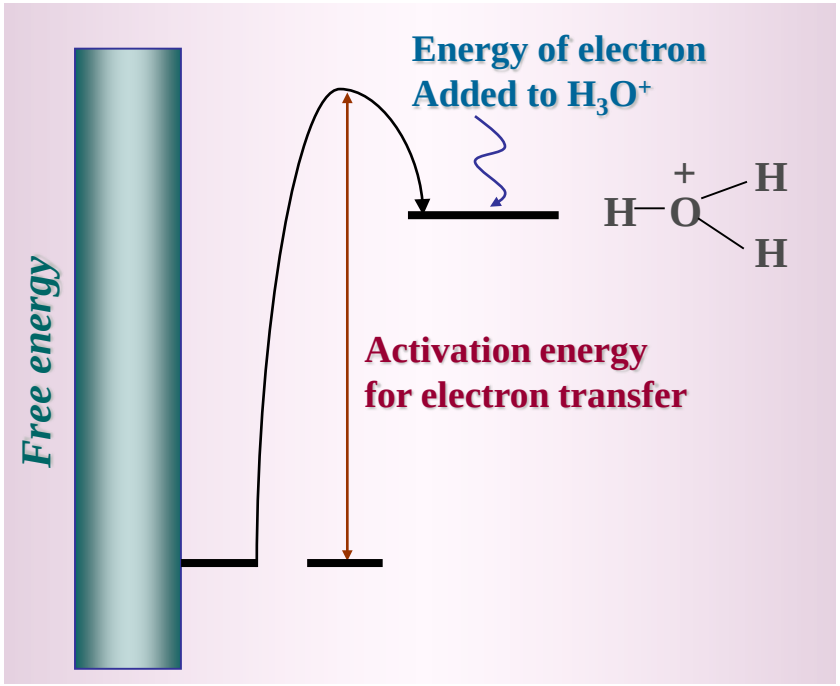

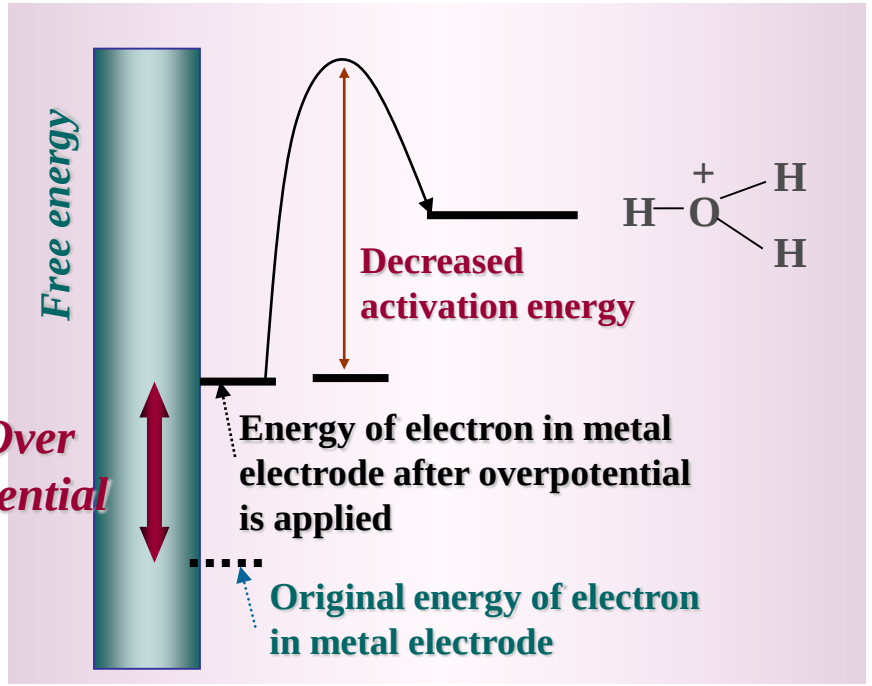

- Fig. 17.5 Schematic energy profile for electron transfer from a metal to H_3O^+ (a) with no applied potential; (b) after a potential is applied to the electrode. The overpotential increases the energy of the electrons in the electrode.

Overpotential

- Table 17.1 Overpotential(V) for gas evolution at various current densities at 25 ℃

Electrode	10 A/m^2		100 A/m^2		1000 A/m^2		10000 A/m^2	
	H_2	O_2	H_2	O_2	H_2	O_2	H_2	O_2
Platinized Pt	0.0154	0.398	0.0300	0.521	0.0405	0.638	0.0483	0.766
Smooth Pt	0.024	0.721	0.068	0.85	0.288	1.28	0.676	1.49
Cu	0.479	0.422	0.584	0.580	0.801	0.660	1.254	0.793
Ag	0.4751	0.580	0.7618	0.729	0.8749	0.984	1.0890	1.131
Au	0.241	0.673	0.390	0.963	0.588	1.244	0.798	1.63
Graphite	0.5995		0.7788		0.9774		1.2200	
Sn	0.8561		1.0767		1.2230		1.2306	
Pb	0.52		1.090		1.179		1.262	
Zn	0.716		0.746		1.064		1.229	
Cd	0.981		1.134		1.216		1.254	
Hg	0.9		1.0		1.1		1.1	
Fe	0.4036		0.5571		0.8184		1.2915	
Ni	0.563	0.353	0.747	0.519	1.048	0.726	1.241	0.853

- **Higher overpotential is required for higher current density (From D. C. Harris Book)**

Potential Ranges

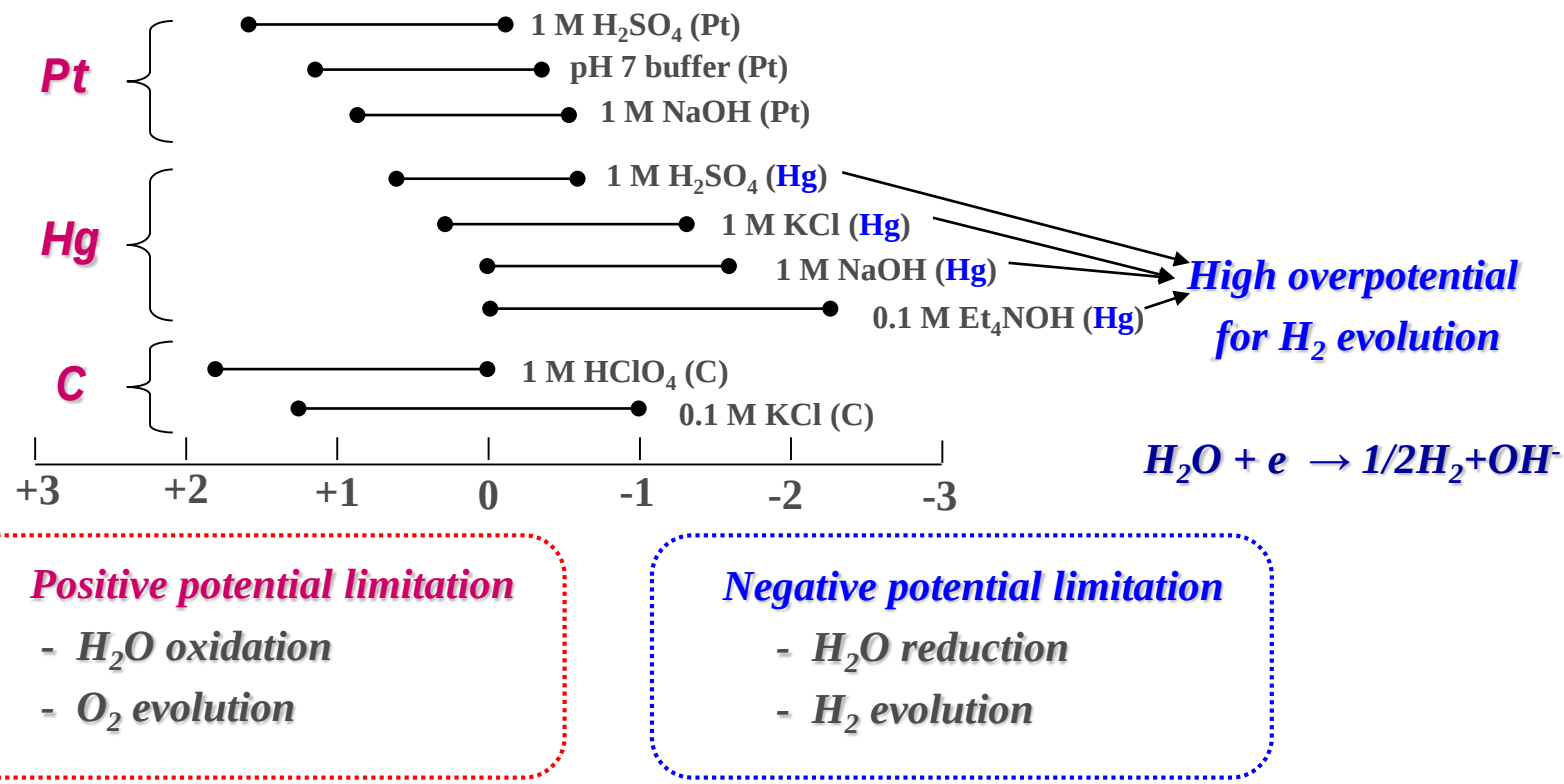

Fig.E.2. **Potential ranges for three types of electrodes in various supporting electrolytes.**
(*Adapted from A. J. Bard and L. R. Faukner*, Electrochemical Methods, *back cover. New York:Wiley 2001*)

Schematic Current-Potential Curve

- Use of Hg electrode
- Addition of a small amount of Cd^{2+}

$$CdBr_4^{2-} + 2e \xrightarrow{Hg} \underline{Cd(Hg)} + 4Br^-$$

Cd^{2+} — *cadmium amalgam*

$$E^0 = -0.35\ V\ vs\ NHE$$

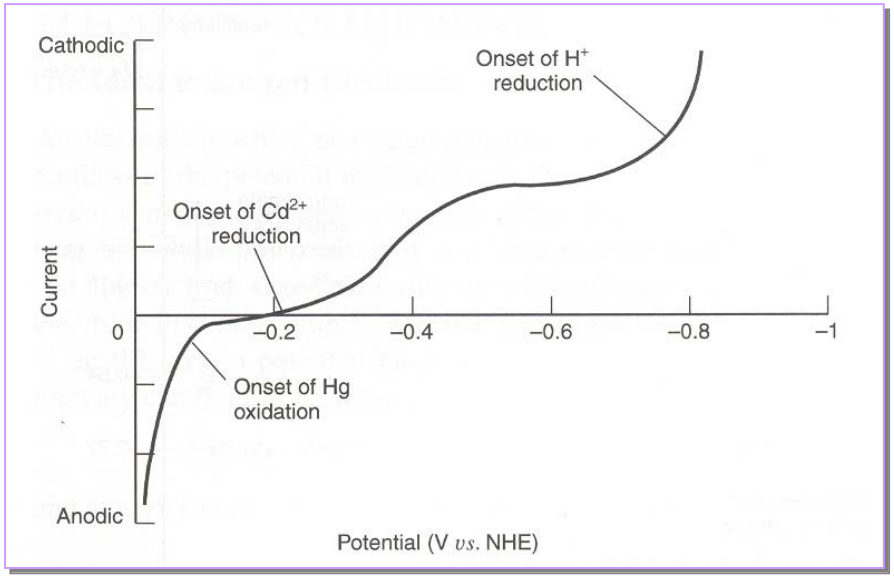

Fig. 1.1.6 Schematic current-potential curve for the Hg electrode in the cell $Hg/H^+, Br^-(1\ M), Cd^{2+}(10^{-3}\ M)/AgBr/Ag$, showing reduction wave for Cd^{2+}.

Predictions for possible Reduction or oxidation

Prediction for possible reduction or oxidation based on thermo-dynamic consideration (E^0)

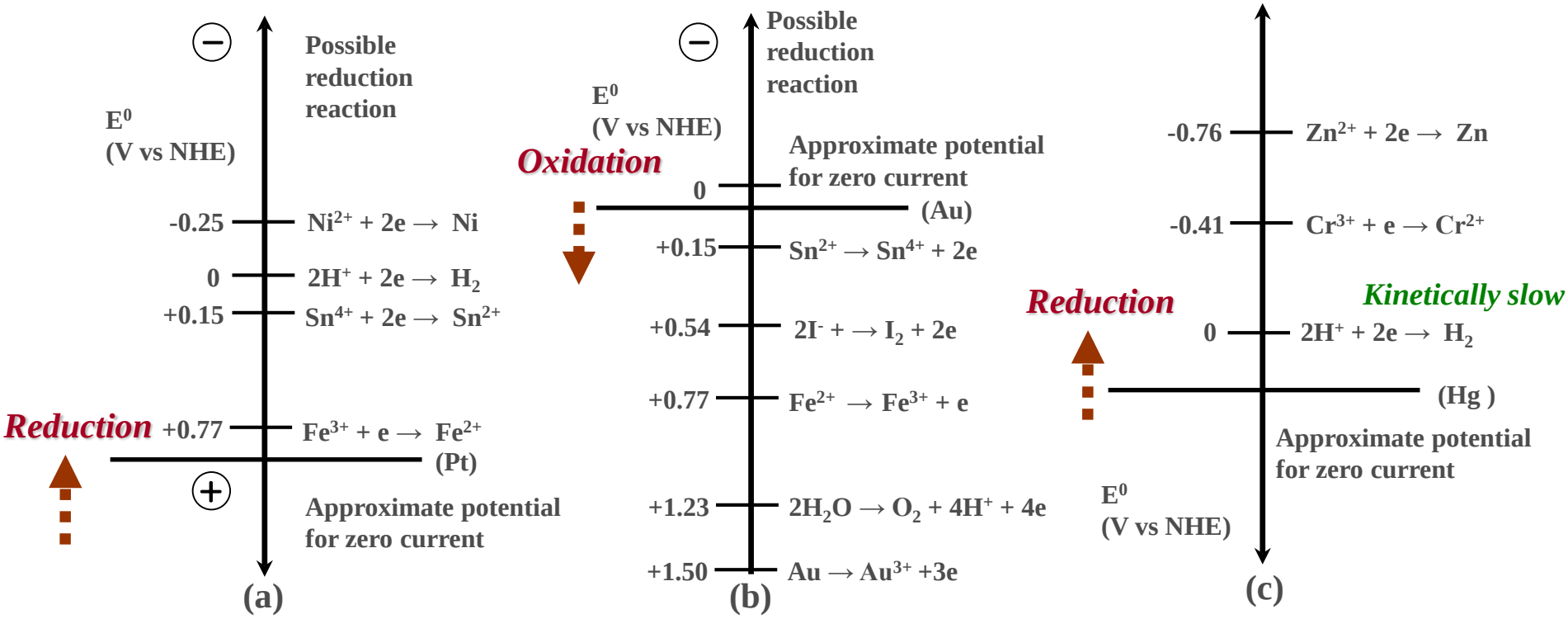

Fig. 1.1.7 (a) Potentials for possible reductions at a platinum electrode, initially at ~1 V vs NHE in a solution of 0.01 M each of Fe^{3+}, Sn^{4+}, and Ni^{2+} in 1 M HCl. (b) Potentials for possible oxidation reactions at a gold electrode, initially at ~ +0.1 V vs. NHE in a solution pf 0.01 M each of Sn^{2+} and Fe^{2+} in 1 M HI. (c) Potentials for possible reductions at mercury electrode in 0.01 M Cr^{3+} and Zn^{2+} in 1 M HCl.

Faradaic and Nonfaradaic Processes

Faradaic Process

- Charge (e.g. electrons) are transferred across the metal-solution interface
- Electron transfer causes oxidation or reduction to occur.
- Such reactions are governed by ***Faraday's Law.***

  The amount of chemical reaction caused by the flow of current is proportional to the amount of electricity passed.

Non-faradaic Process

- Adsorption and desorption
- The electrode-solution interface can change with changing potential or solution composition.
- Although charge does not cross the interface, external currents can flow (at least transiently)

Electrode – Solution Interface (electrical double layer)

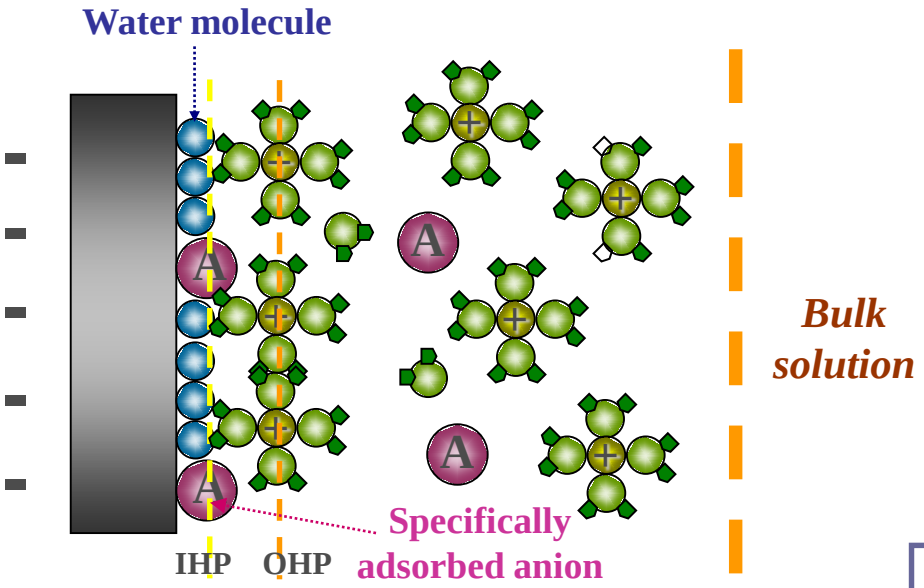

<Bockris-Devanathan-Müller Model>

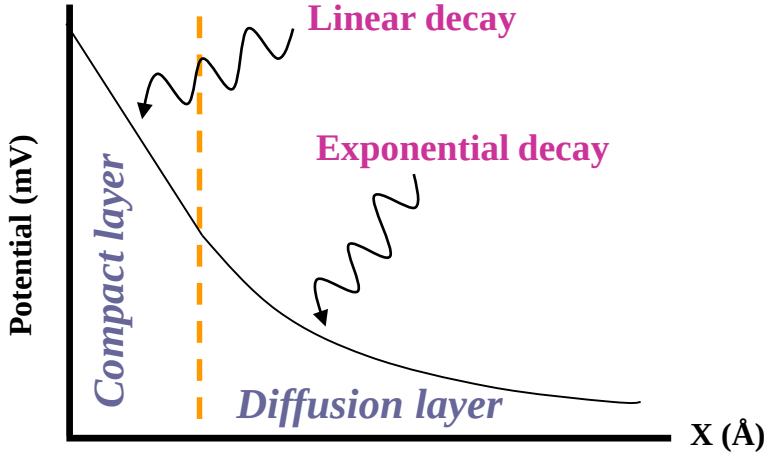

Three models of electrical double layer

- Helmholtz model (1879)
- Diffuse double layer model (Guoy-Chapman) model
- Stern model

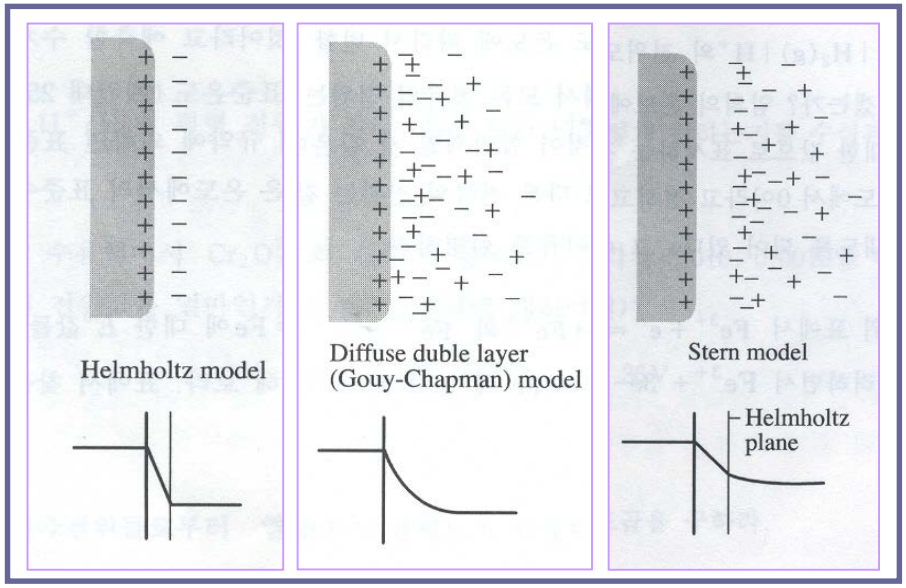

Simplified Model

Faradaic current

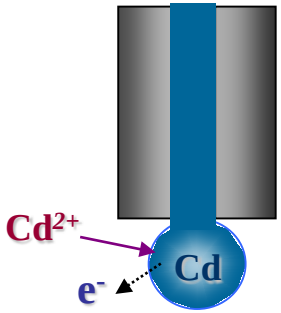

Charging current

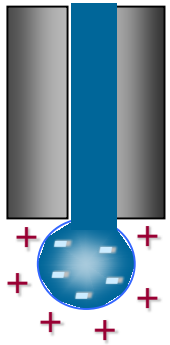

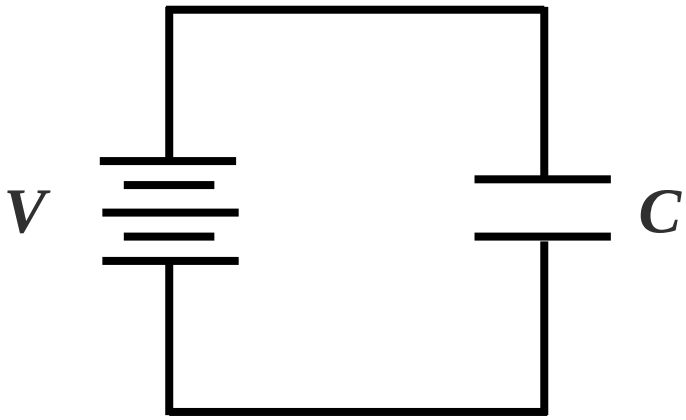

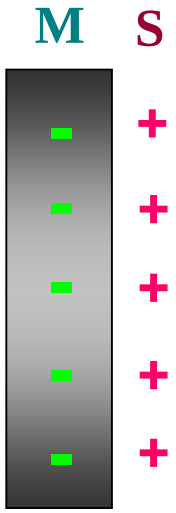

$-q_M = q_s$

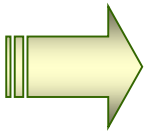

Capacitor

- C_d *(double layer capacitance)*
  - very small charge
  - μc/cm², 10 ~ 100 μF/cm²

$C_d = q/E$

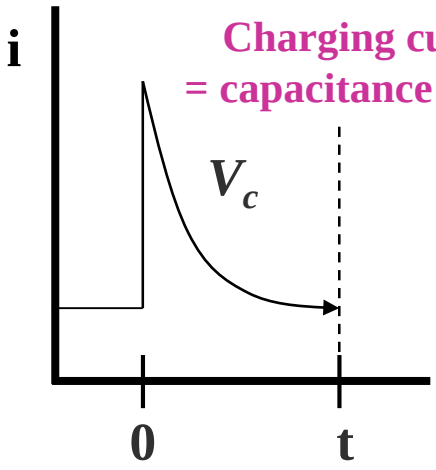

Voltage (Potential) Step

$$q = C_d \cdot E_C$$

$$E = E_R + E_C = iRs + \frac{q}{C_d} \quad \left(i = \frac{dq}{dt} \text{ 이므로 } \right)$$

$$\Rightarrow \frac{dq}{dt} = \frac{E}{R_s} - \frac{q}{R_s C_d} \quad \text{-------} \ (1)$$

Initially, capacitor is uncharged q = 0 at t = 0

$$q = E\, C_d \left[1 - e^{-t / RsCd} \right] \quad \text{-------} \ (2)$$

$$i = \frac{E}{R_s} e^{-t / RsCd}$$

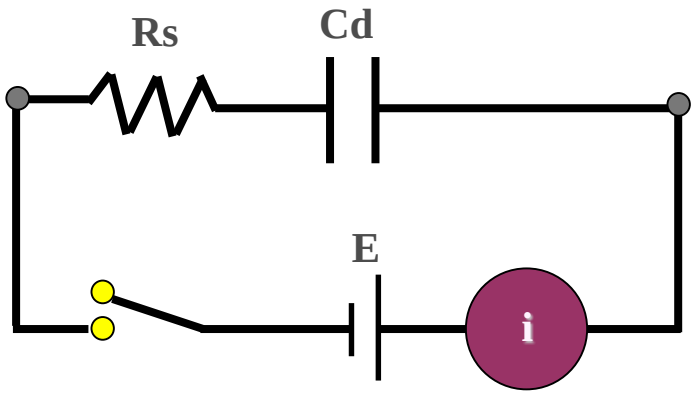

Fig. 1.2.6 Potential step experiment for an RC circuit.

Voltage (Potential) Step

- For a potential step input, there is an exponentially decaying current having a time constant, $\tau = R_s \cdot C_d$.
- Double-layer charging current drops to 37 % of its initial value at $t = \tau$, 5 % at $t = 3\tau$.

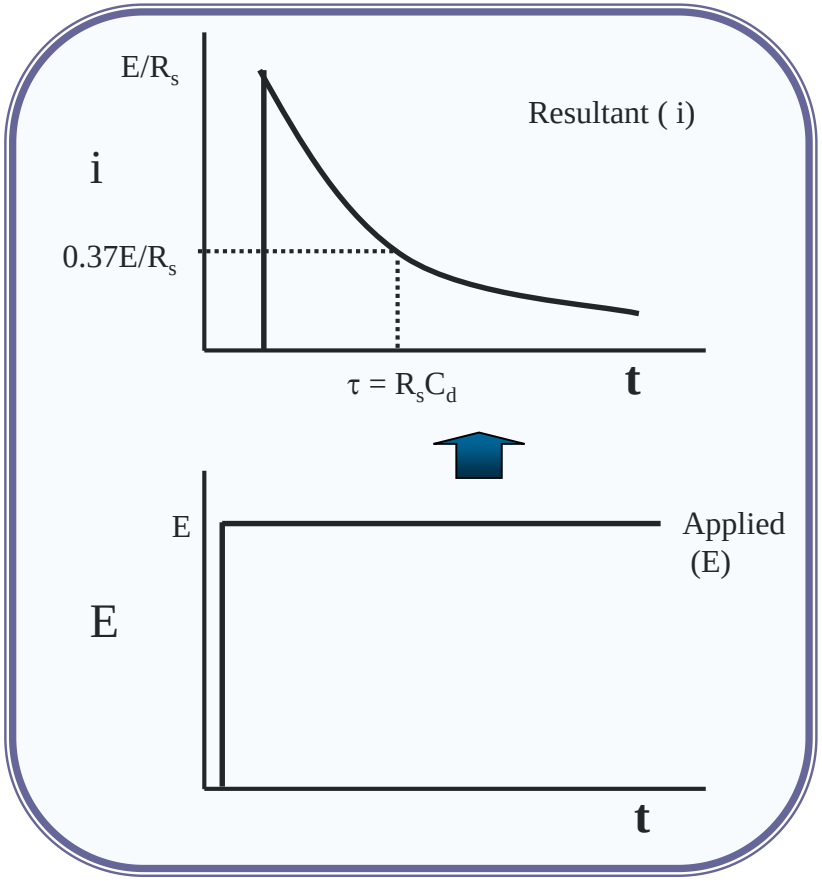

- if Rs = 1 Ω, Cd = 20 μF

↓

τ = 20 μs

at 60 μs 95 % complete

Fig. 1.2.7 Current transient (I vs. t) resulting from a potential step experiment .

Voltage Ramp (or potential sweep)

Linear Potential Sweep

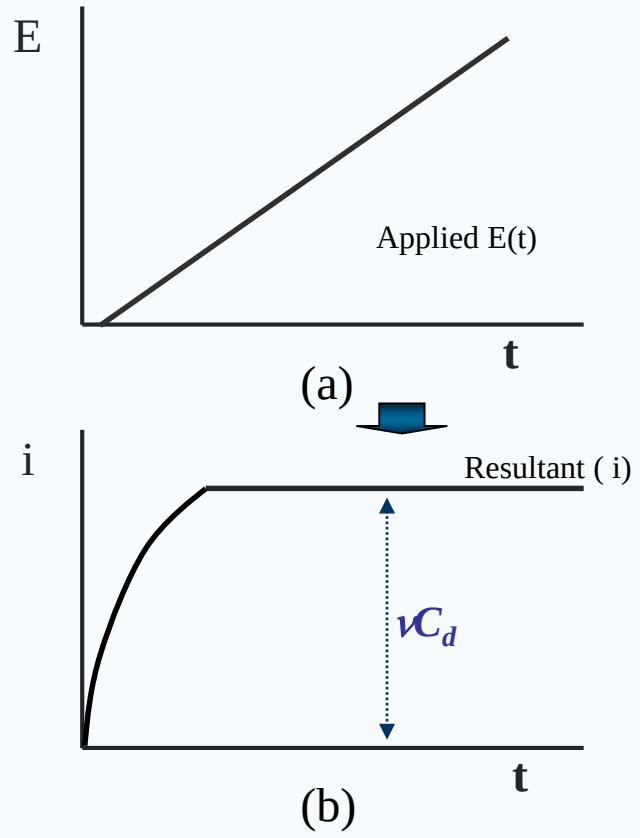

Fig. 1.2.10 Current –time behavior resulting from a linear potential sweep applied to an RC circuit .

ν (in V/s)

Current rises from zero to a steady-state Value, νC_d

$$E = \nu t$$

$$E = iR_s + \frac{q}{C_d} \quad \text{에서}$$

$$\nu t = \left(\frac{dq}{dt}\right) R_s + \frac{q}{C_d}$$

If q = 0 at t = 0,

$$i = \nu C_d \left[1-\exp(-t/R_s C_d)\right]$$

Voltage Ramp (or potential sweep)

Cyclic Potential Sweep

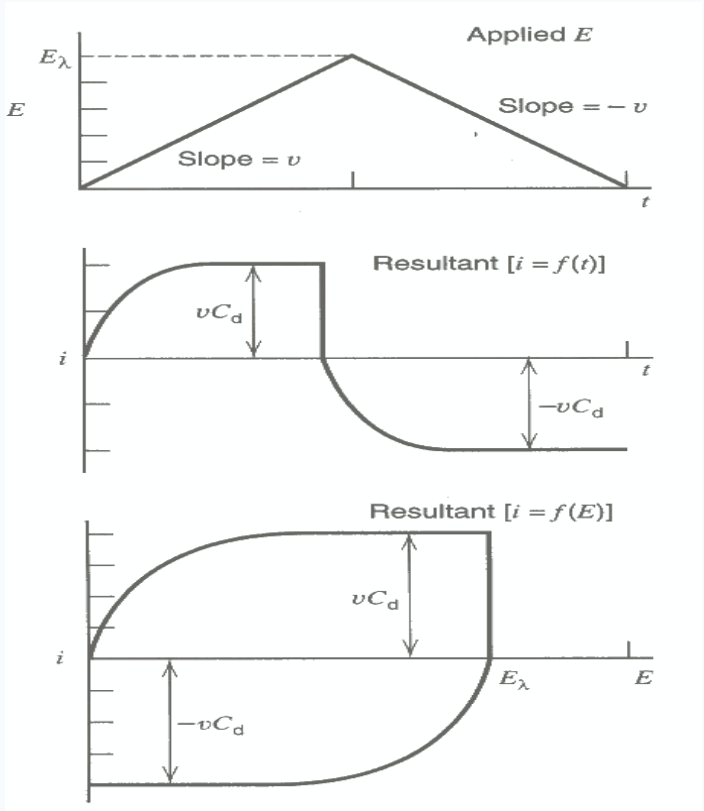

Fig. 1.2.11 Current –time and current-potential plots resulting from a cyclic linear potential sweep (or triangular wave) applied to an RC circuit.

From CV, we can get C_d

전극 면적에 의존

$$C_d = \left(\frac{\text{Charging current}}{\nu \text{ (scan rate)}} \right)$$

Factors affecting electrode reaction rate and current

Heterogeneous at the electrode/electrolyte interface

Rate depends on...

- Mass transfer to the electrode
- Surface effects (or reaction) : adsorption / desorption, crystallization
- Kinetic variables (electron transfer)

Considering electrode area

$$\text{Rate } (mol \cdot s^{-1} \cdot cm^{-2}) = \frac{i}{nFA} = \frac{j}{nF}$$

current density (i/cm^2)

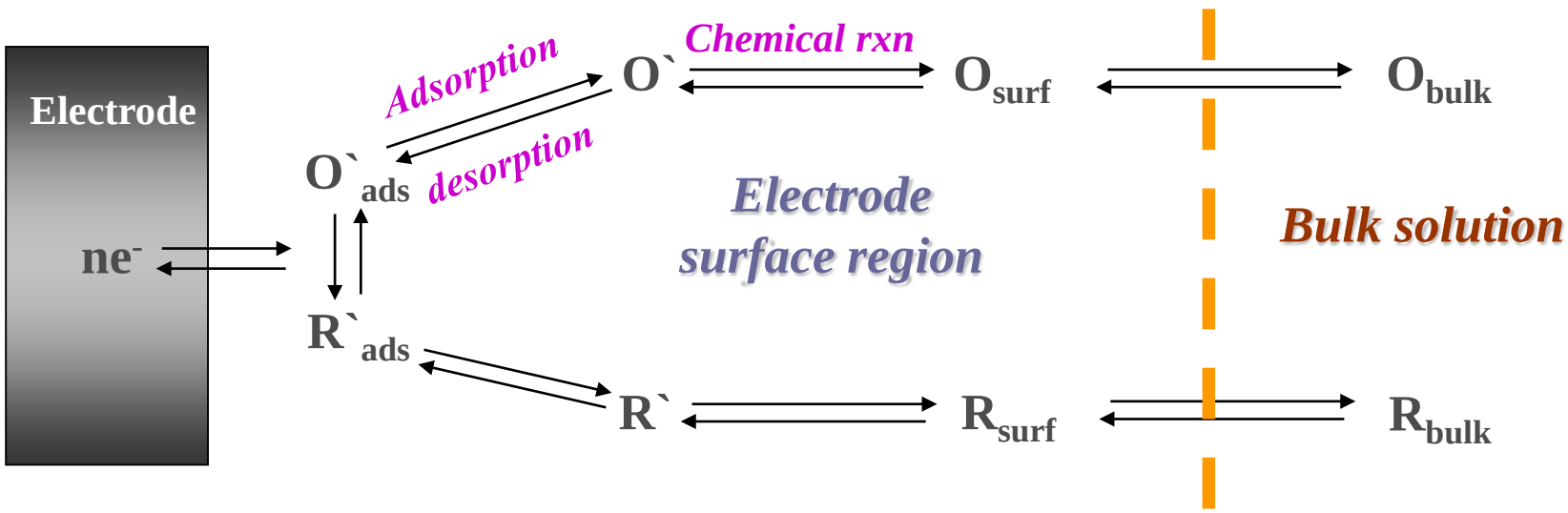

Mechanisms of Mass Transport

- The electrochemical reduction/oxidation of a molecule occurs at the electrode-solution interface.
- A molecule dissolved in solution in an electrochemical cell must be transported to the electrode surface for the electrochemical event to occur.
- The transport of molecules from regions in the solution phase to the electrode surface is an important aspect of many electrochemical techniques.
- The movement of material from one place to another is generally termed mass transport or mass transfer.

Hydrodynamic movement (convection)

- Transport of dissolved chemical species by physical movement of the solution or the electrode relative to each other.
  - stirring the solution
  - rotating the electrode
  - flowing solution across the electrode by placing it in a tube through which solution is pumped.

Mechanisms of Mass Transport

Diffusion

- A process of spatial movement of ions or molecules due to their kinetic motion (random Brownian motion)
- Diffusion acts to remove a concentration gradient by the mass transport of molecules from a region of high concentration to a region of low concentration.
- Diffusion increases the entropy of a system.

Concentration profile

$$C_{x,t} = \frac{C_0}{(4\pi Dt)^{1/2}} \exp\left(\frac{-x^2}{4Dt}\right)$$

- $C_{x,t}$: concentration of solute molecules at x, t ($mol \cdot cm^{-3}$)
- C_0 : concentration of solute molecules at initial impulse
- x : distance from center of impulse (cm)
- D : diffusion coefficient (cm^2/s)

Mechanisms of Mass Transport

- **Diffusion Distance**

$$\sigma = \sqrt{2Dt}$$

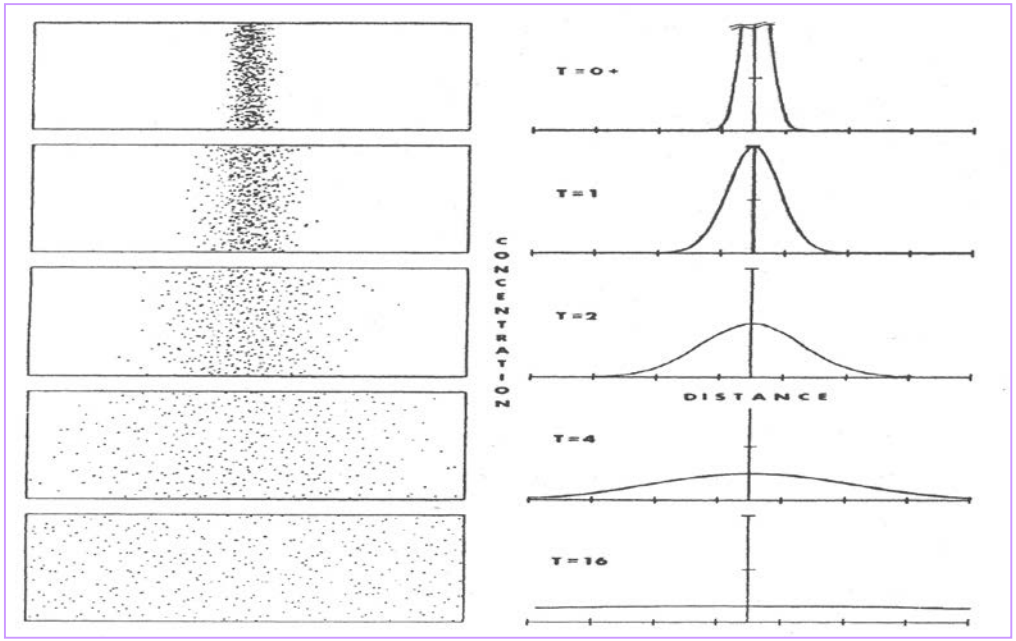

Migration

- **Movement of charged particles under the influence of electric field.**

  (e.g) positively charged electrode attracts a negatively charged solute species, but repels a positively charged solute species.

Potential excitation signal used in voltammetry

Linear scan

Polarography linear -scan voltammetry

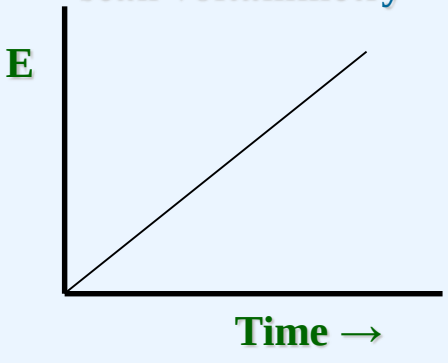

Differential pulse

Differential pulse Polarography

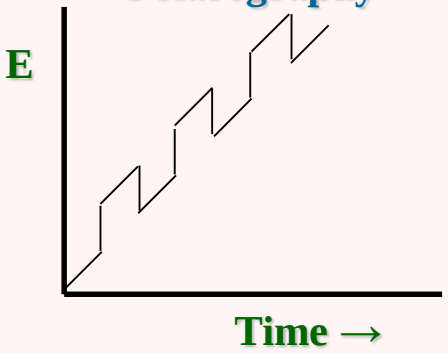

Square wave

Square-wave voltammetry

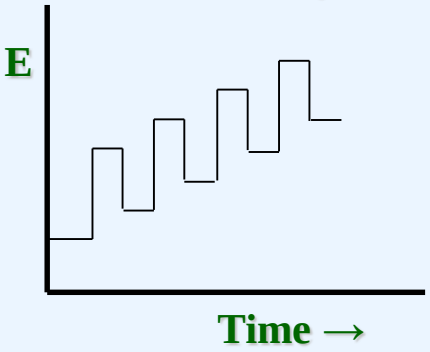

Triangular

Cyclic voltammetry

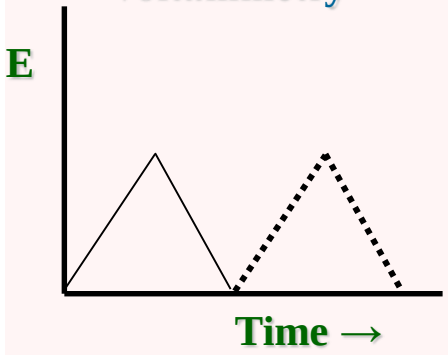

Pulse

Pulse voltammetry

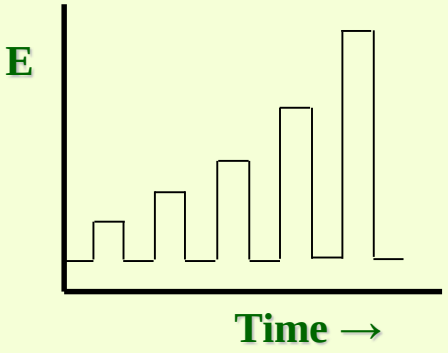

Staircase

Staircase voltammetry

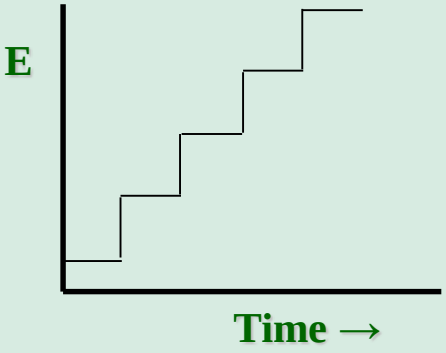

Constant

LCEC Amperometry
Deposition in ASV controlled E coulometry

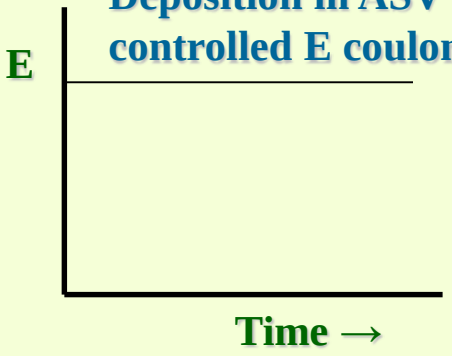

Cyclic Voltammtry(CV) : no stirring

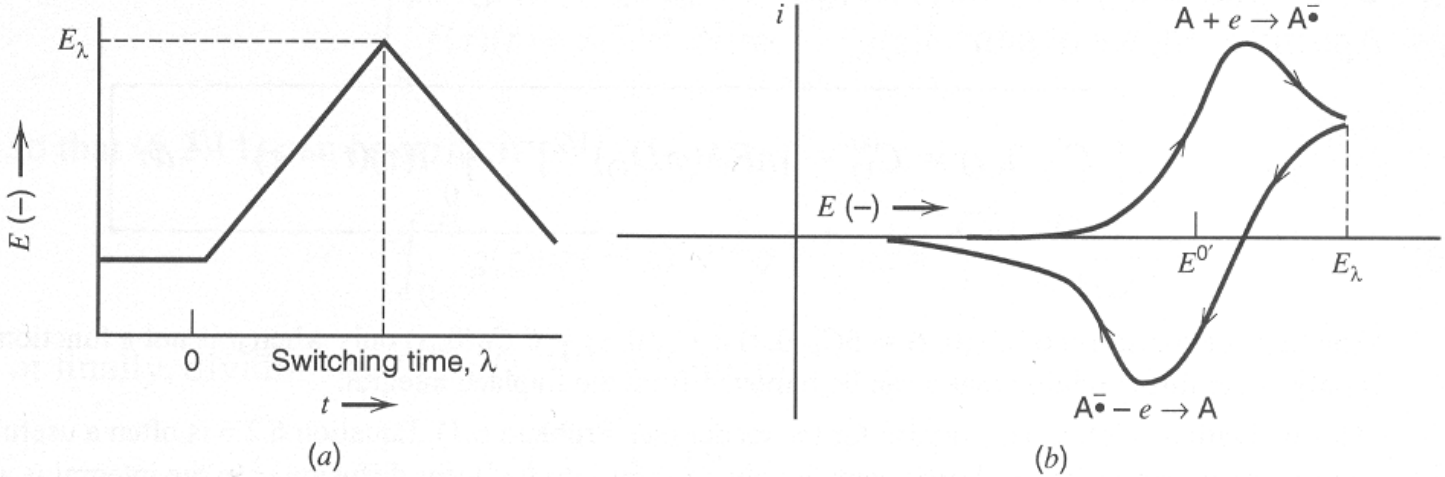

Figure 6.1.3 (*a*) Cyclic potential sweep. (*b*) Resulting cyclic voltammogram.

- **CV:** very popular technique for initial electrochemical studies of new systems

Cyclic Voltammtry(CV)

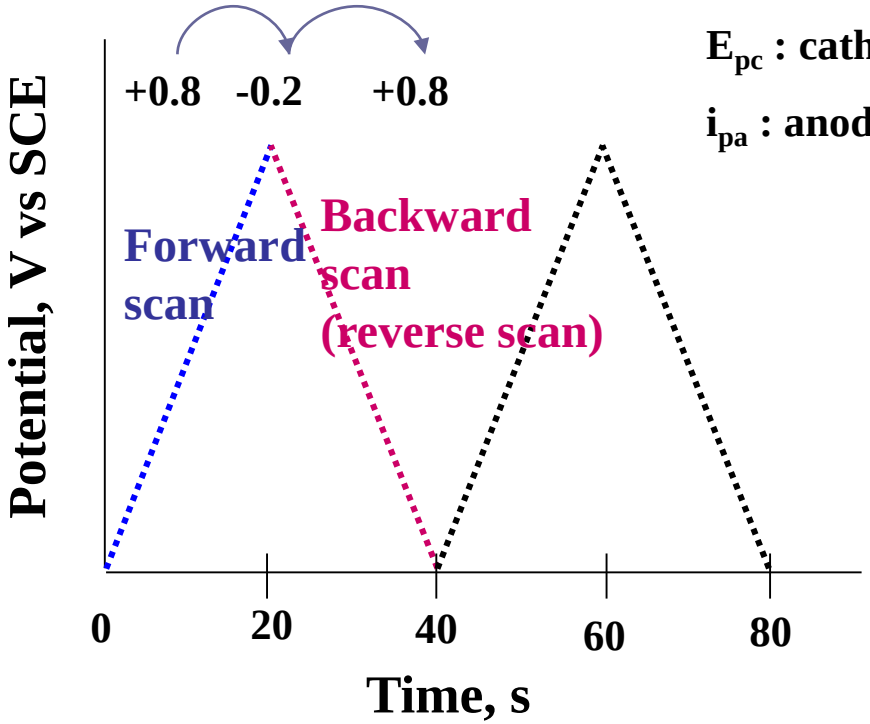

Scan rate = V/s

: 1.0 V/20 s = 50 mV/s

- Figure. Cyclic voltammetric excitation signal used to obtained voltammogram in Figure 25-20.

E_{pc} : cathodic peak potential, E_{pa} : anodic peak potential

i_{pa} : anodic peak current, i_{pc} : cathodic peak current

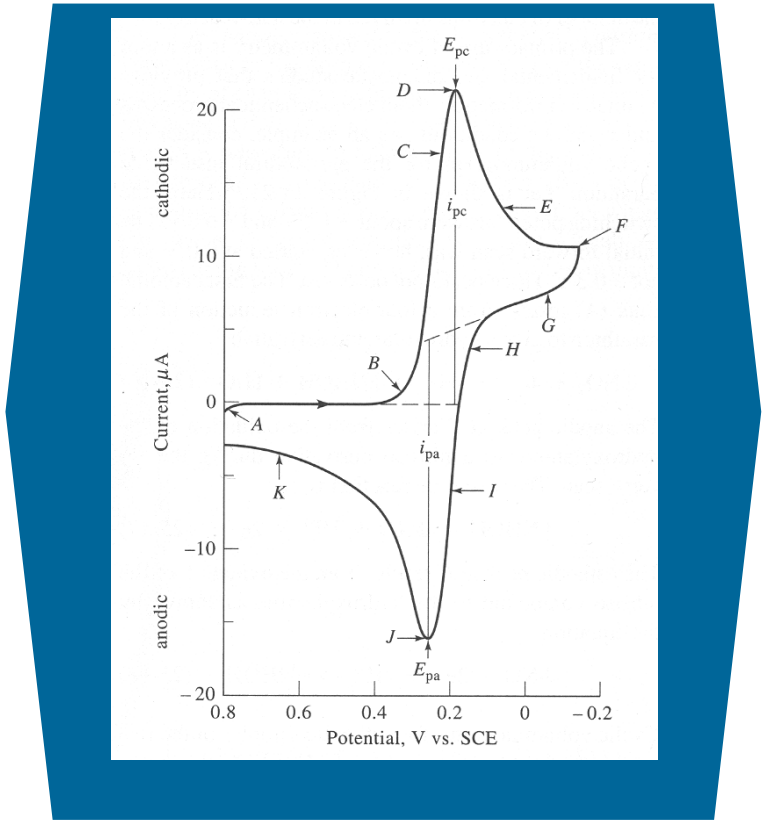

- Figure 25. 20 Cyclic voltammogram for a solution that is 6.0 mM in $K_3Fe(CN)_6$ and 1.0 M in KNO_3.

Cyclic Voltammtry(CV)

- Nernst Equation for a Reversible System at 25 ℃

$$E = E^{o'}_{Fe3+,\,Fe2+} - \frac{0.0591}{n} \log \frac{C^s(Fe^{2+})}{C^s(Fe^{3+})}$$

At point C, $E=E^{o'}$

$$\frac{C^s(Fe^{2+})}{C^s(Fe^{3+})} = 1$$

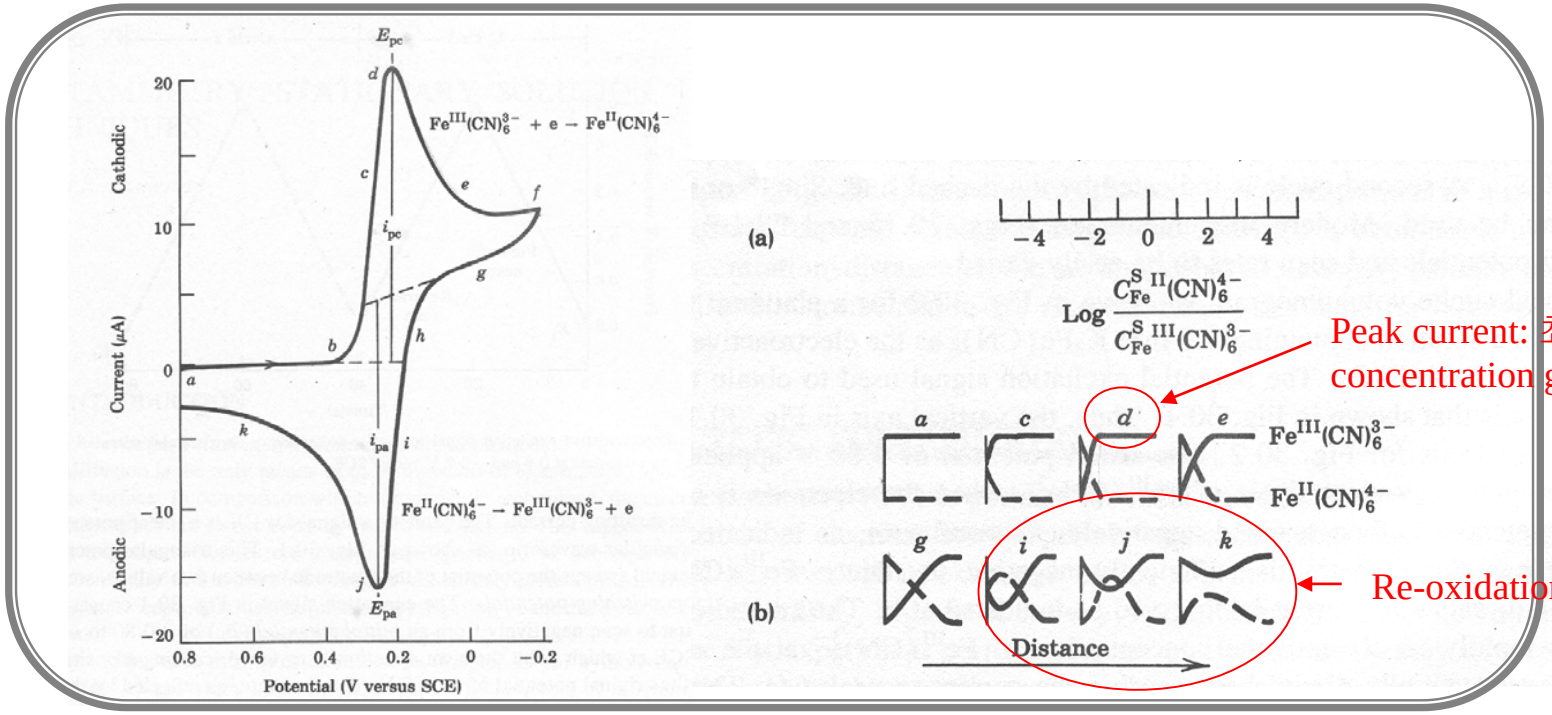

- **Figure (a) Cyclic voltammogram of 6 mM $K_3Fe(CN)_6$ in 1 M KNO_3. Scan initiated at 0.8 V versus SCE in negative direction at 50 mV/s. Platinum electrode, A=2.54 mm^2. (b) Concentration-distance(C-x) profiles a-k keyed to voltammogram.**

Cyclic Voltammtry(CV)

- Peak current for a reversible system the working electrode (**Randles-Sevcik equation**)

$$i_p = (2.69 \times 10^5)\, n^{3/2} A D^{1/2} C^* v^{1/2}$$

A : electrode area, D : diffusion coefficient

C* : bulk concentration (mol ·cm^{-3})

v : scan rate (V · s^{-1})

- $i_p \propto v^{1/2}$
  from slope D can be calculated

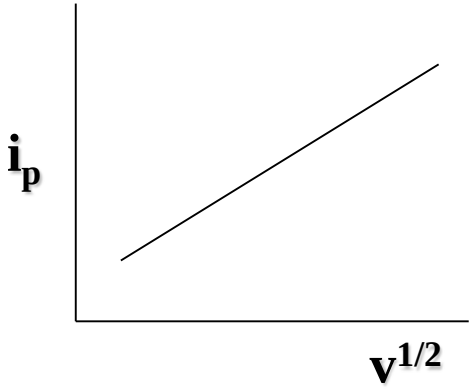

Cyclic Voltammtry(CV): Scan Rate Effect

The slope of the concentration distance profile at the electrode surface

$$i = nFADo \left[\frac{\partial Co}{\partial x}\right]_{x=0,\ t} = nFADo \frac{Co - Co^{s}}{\delta}$$

δ Diffusion layer distance

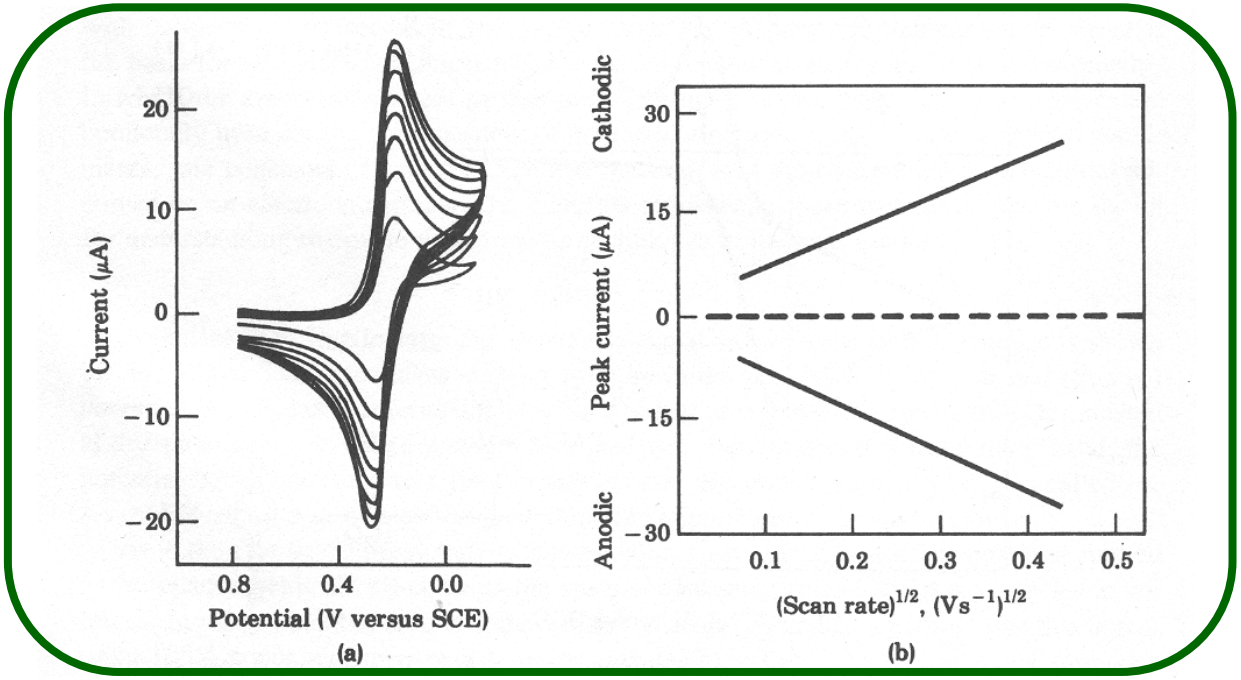

Figure 30.3 (a) Effect of variation of scan rate on cyclic voltammograms and (b) plot of ip versus $v^{1/2}$.

Cyclic Voltammetry for Reversible System

For reversible redox couple:

$E^{o'} = (E_{pa} + E_{pc}) / 2$: formal potential

- Peak separation $\Delta E_p = E_{pa} - E_{pc} = 59\ mV/n$

실제로 switching potential(Eλ)에 따라 약간씩 변한다.

⇨ the number of electrons transferred in the electrode reaction(n) for a reversible couple can be determined from the separation between peak potential at 25 ℃.

For $Fe(CN)_6^{3-} \rightarrow Fe(CN)_6^{4-}$ ΔE_p = 0.059 V (n=1)

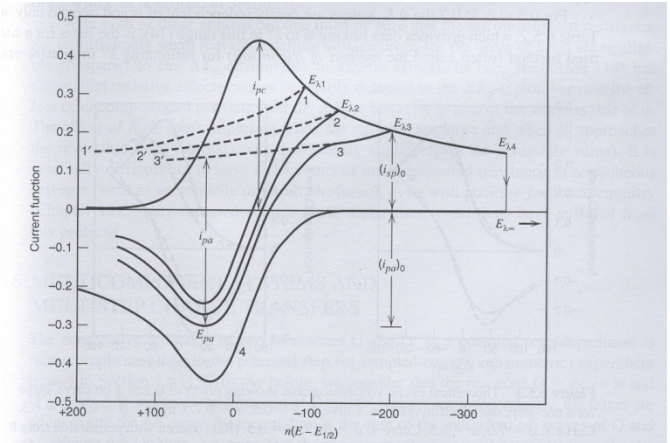

Figure 6.5.2 Cyclic voltammograms under the same conditions as in Figure 6.5.1, but in an *i-E* format. E_λ of (*1*) $E_{1/2} - 90/n$; (*2*) $E_{1/2} - 130/n$; (*3*) $E_{1/2} - 200/n$ mV; (*4*) for potential held at $E_{\lambda 4}$ until the cathodic current decays to zero. [Curve 4 results from reflection of the cathodic *i-E* curve through the *E* axis and then through the vertical line at $n(E - E_{1/2}) = 0$. Curves 1, 2, and 3 result by addition of this curve to the decaying current of the cathodic *i-E* curve (1′, 2′, or 3′).]

Table 6.5.1 Variation of ΔE_p with E_λ for a Nernstian System at 25°C (3)

$n(E_{pc} - E_\lambda)$ (mV)	$n(E_{pa} - E_{pc})$ (mV)
71.5	60.5
121.5	59.2
171.5	58.3
271.5	57.8
∞	57.0

Cyclic Voltammtry(CV)

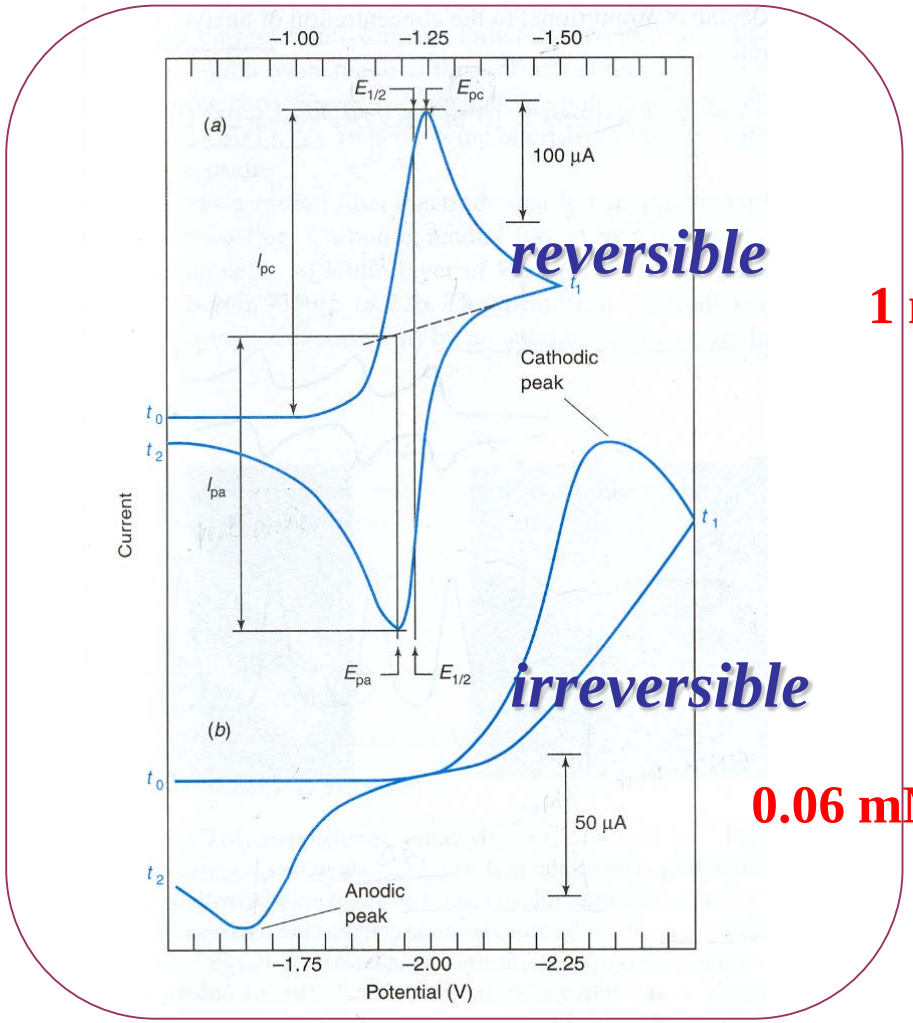

1 mM O_2

0.06 mM 2-nitropropane

"Reversible" means the reaction is fast enough to maintain equilibrium concentrations of the reactant and product *at the electrode surface*

UltraMicroelectrode(~μm diameter)

- small size (implantable)
- small iR drop (useful in resistive and nonaqueous media
- small charging current (high fast scan possible, high sensitivity)

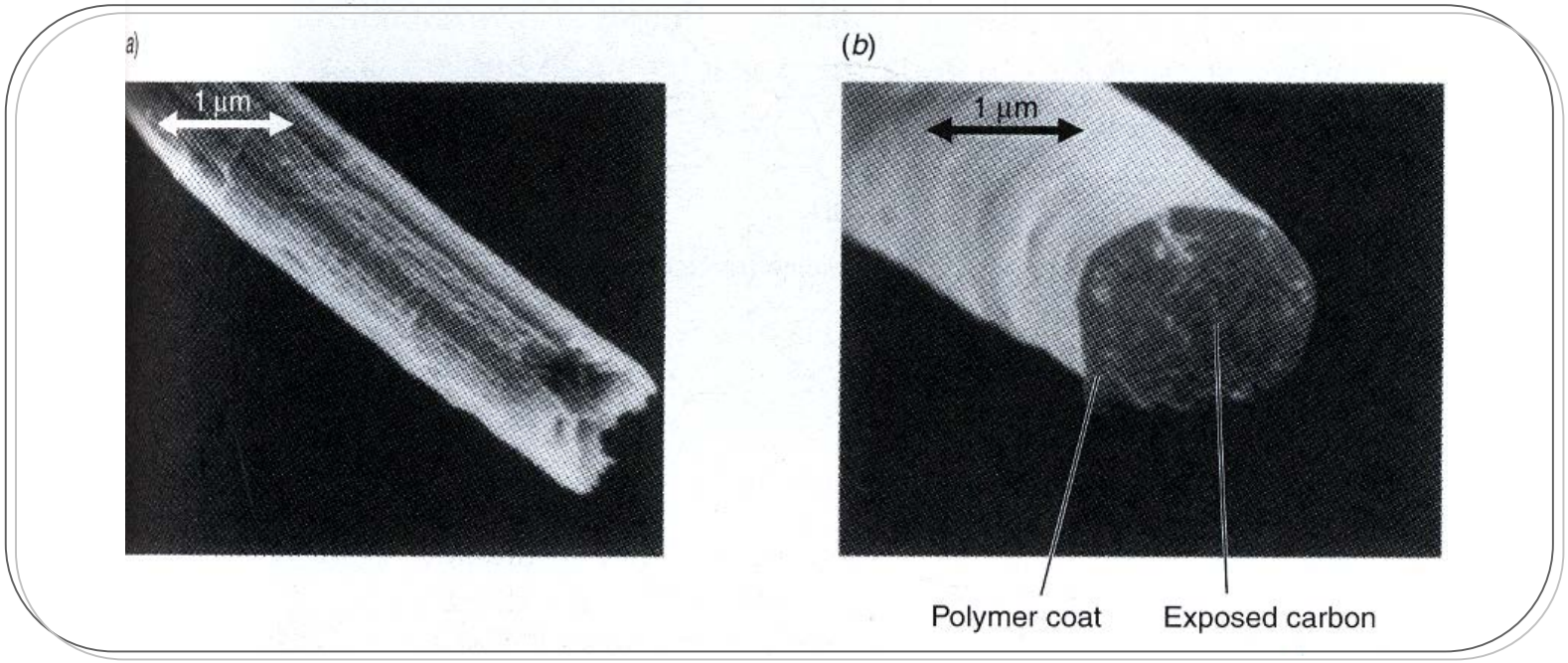

Figure 18.22 (a) scanning electron micrograph of a carbon fiber that has been etched to ~1μm diameter by drawing through a flame. (b) Carbon fiber with thin, insulating coating formed by electrolytic copolymerization of phenol and 2-alkylphenol. Once coated, the tip of the fiber is the only electrochemically active surface.

Cyclic Voltammetry with UME

Fast scan: linear diffusion dominates **Slow scan: radial diffusion dominates**

Ferrocene Oxidation

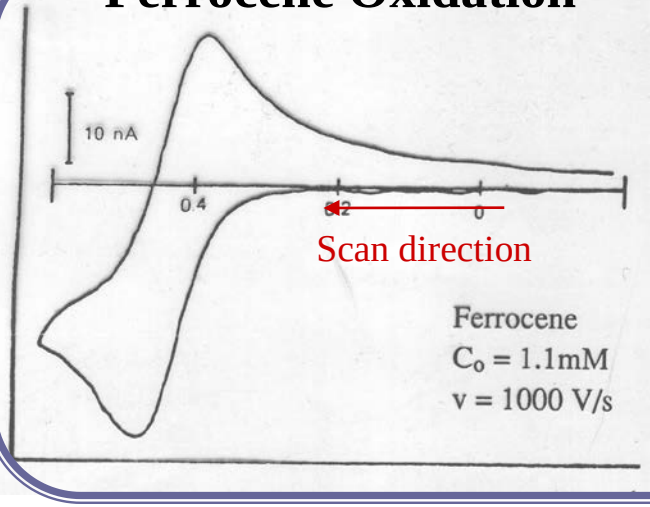

$$\frac{1}{\sqrt{\pi Dt}}$$

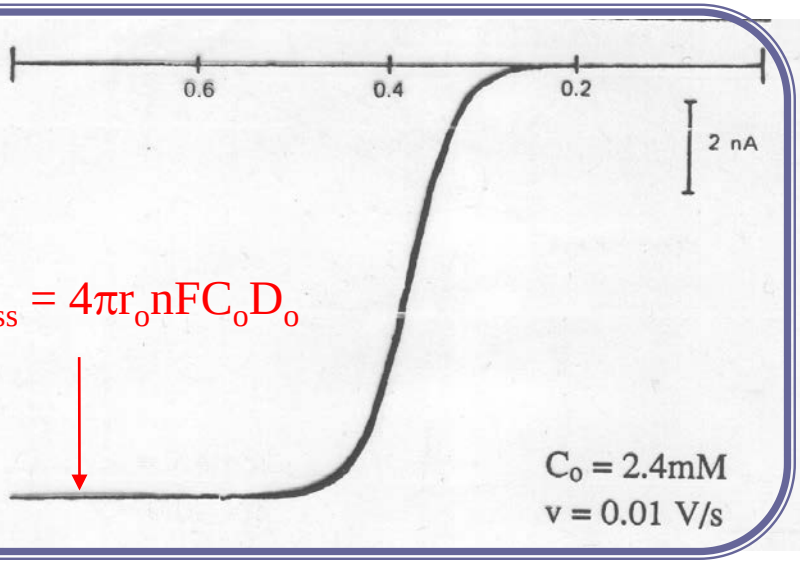

$Ru(NH_3)_6^{3+}$ reduction

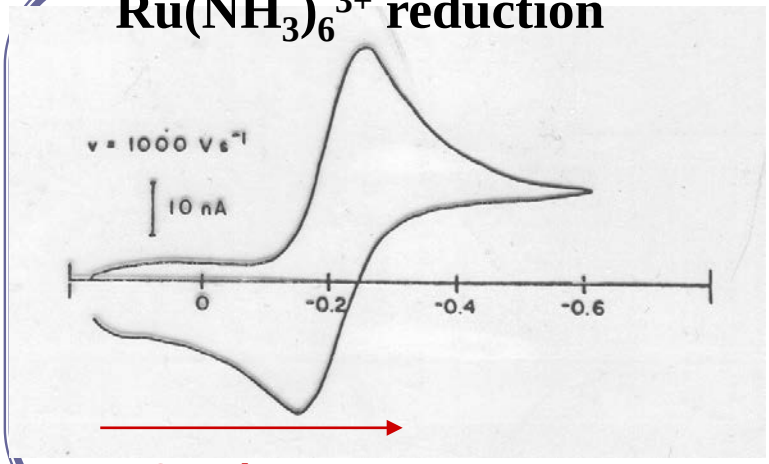

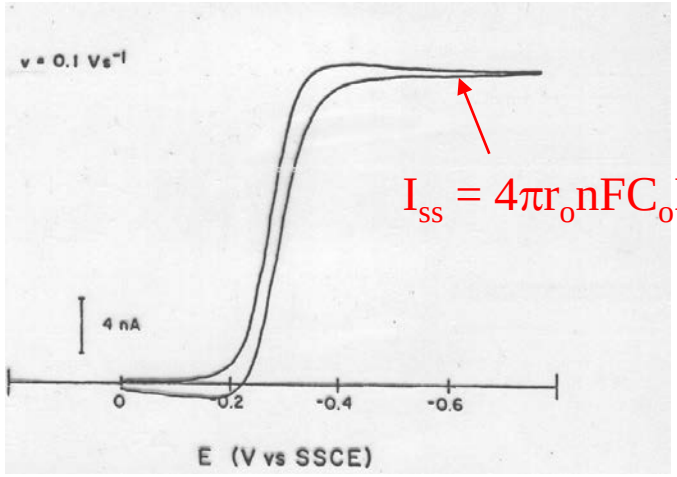

Amperometry (i vs time) at fixed potential

Stirring

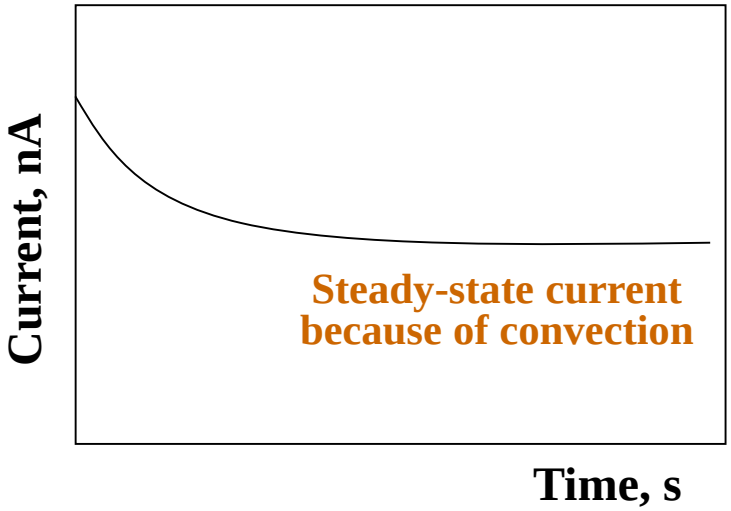

Figure 3.13 Current measured during an amperometric experiment. A constant potential(-700 mV) as a function of time is applied to a plamar Au electrode in PBS saturated with air.

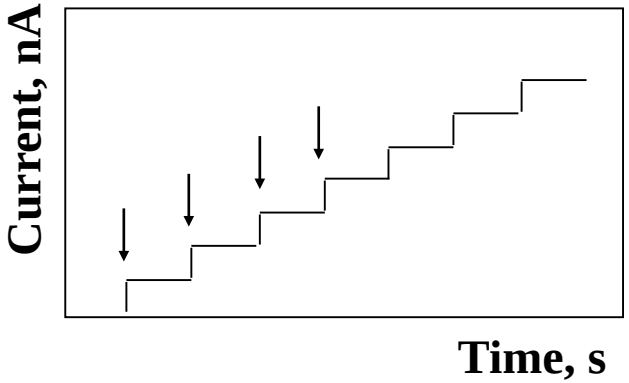

Figure 6.18 Amperometric response of a thick-film RuO_2 electrode to step-wise changes of the H_2O_2 concentration in a stirred PBS solution.

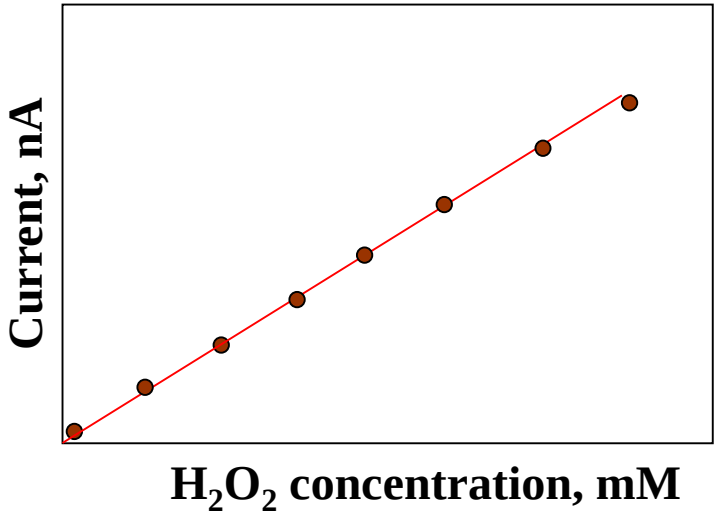

Calibration curve obtained from the measurement in figure 6.18.

Oxygen Electrode

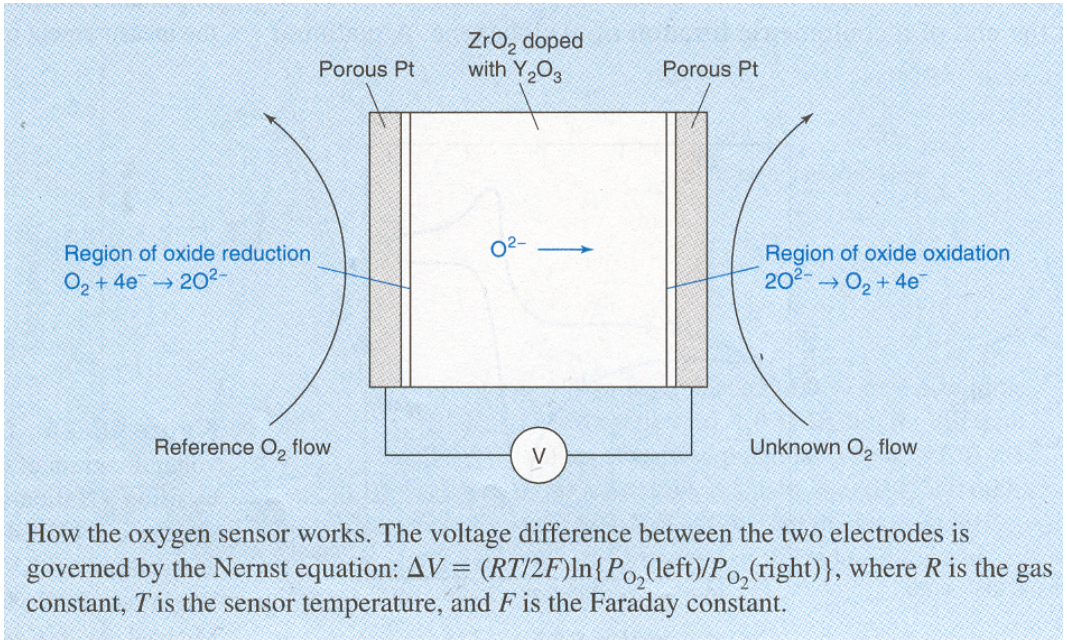

How the oxygen sensor works. The voltage difference between the two electrodes is governed by the Nernst equation: $\Delta V = (RT/2F)\ln\{P_{O_2}(\text{left})/P_{O_2}(\text{right})\}$, where R is the gas constant, T is the sensor temperature, and F is the Faraday constant.

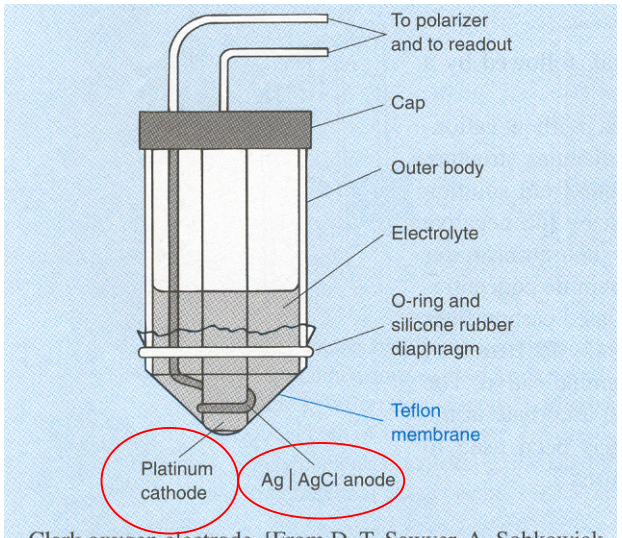

Clark oxygen electrode. [From D. T. Sawyer, A. Sobkowiak, and J. L. Roberts, Jr., *Electrochemistry for Chemists,* 2nd ed. (New York: Wiley, 1995).]

- **Clark Electrode : Pt cathode held at -0.6 V vs Ag/AgCl**

  cathode : $O_2 + 4H^+ + 4e^- \leftrightarrow 2H_2O$

  anode : $2Ag + 2Cl^- \leftrightarrow 2AgCl + 2e^-$

Glucose Biosensor based on Clack Electrode

Biosensor (Amperometric)

Limiting factor

$$\text{Glucose} + O_2 \rightarrow H_2O_2 + \text{gluconic acid}$$

$$H_2O_2 + OH^- \leftrightarrow O_2 + H_2O + 2e^-$$

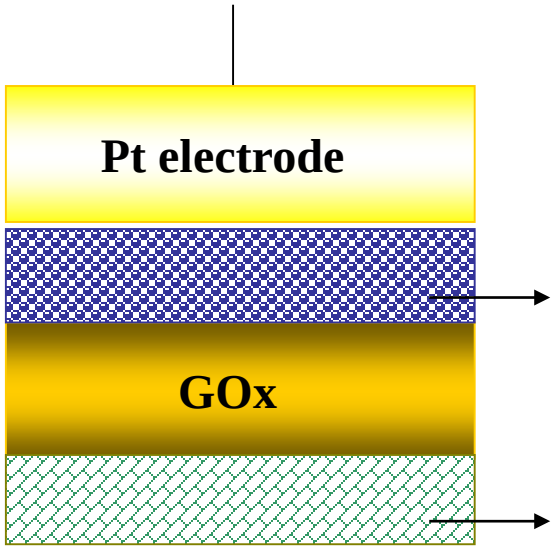

Cellulose acetate membrane
: permeable to small molecules H_2O_2

Polycarbonate film
: permeable to glucose
: impermeable to proteins and other constituents in blood

- 1st generation : O_2 electrode (stoichiometric limitation)
- 2nd generation : H_2O_2 detection(interference) 0.5 vs Ag/AgCl

Mediators

Glucose Biosensor

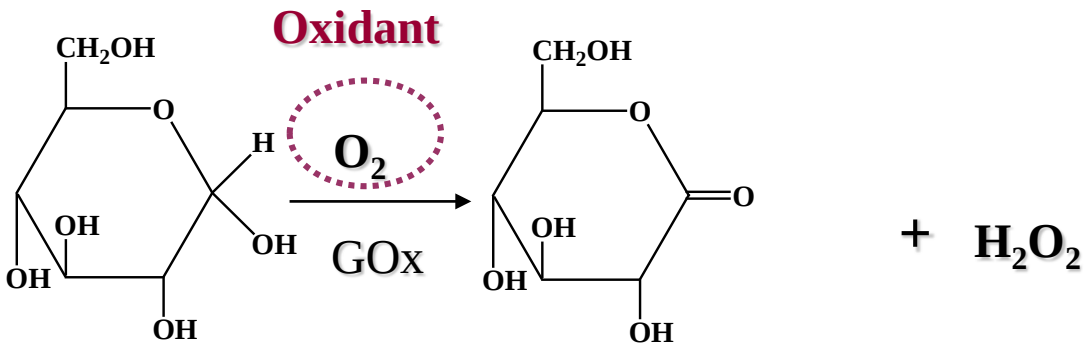

Glucose Gluconolactone

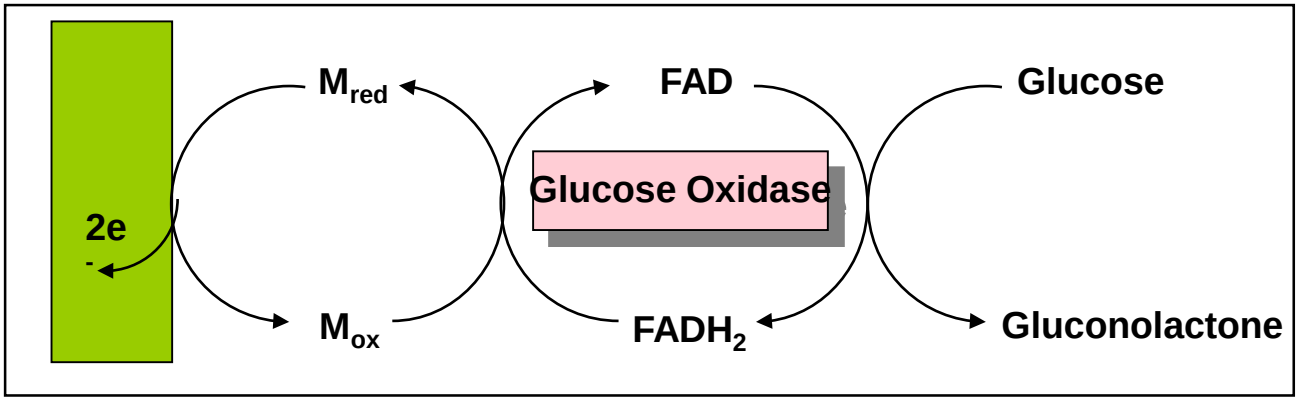

A.E.G. Cass, et. al., *Anal. Chem.*, **1984**, *56*, 667-671

Electron Transport Mediator

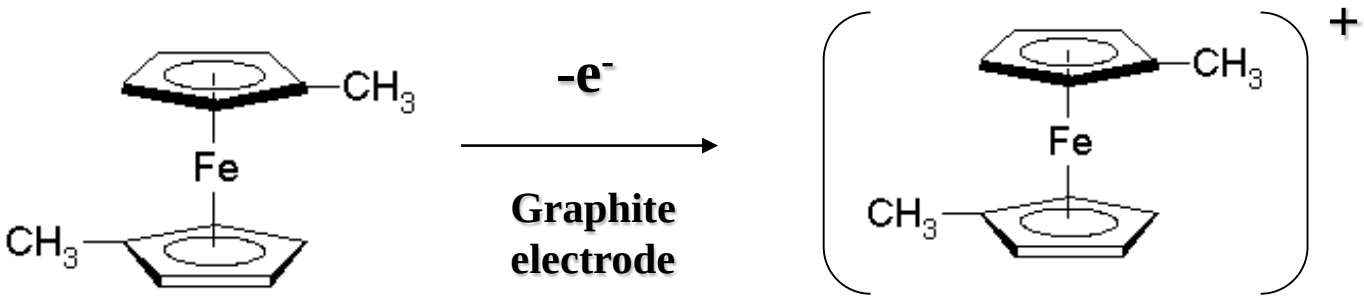

1,1'-Dimethylferrocene 1,1'-Dimethylferricinium cation

Enzyme-Linked Immunosorbent Assay (ELISA)

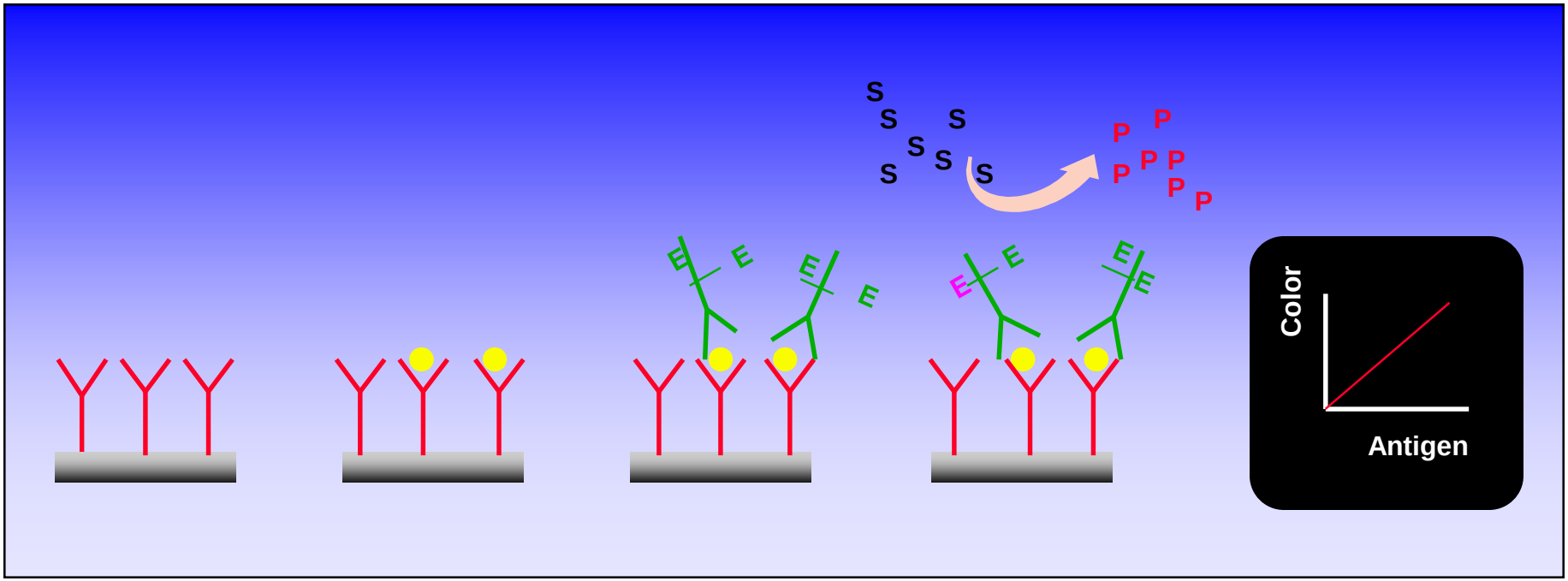

Antibody

Antigen

Secondary antibody

S Substrate (colorless)

P Product (colored)

Amperometric Immunoassay

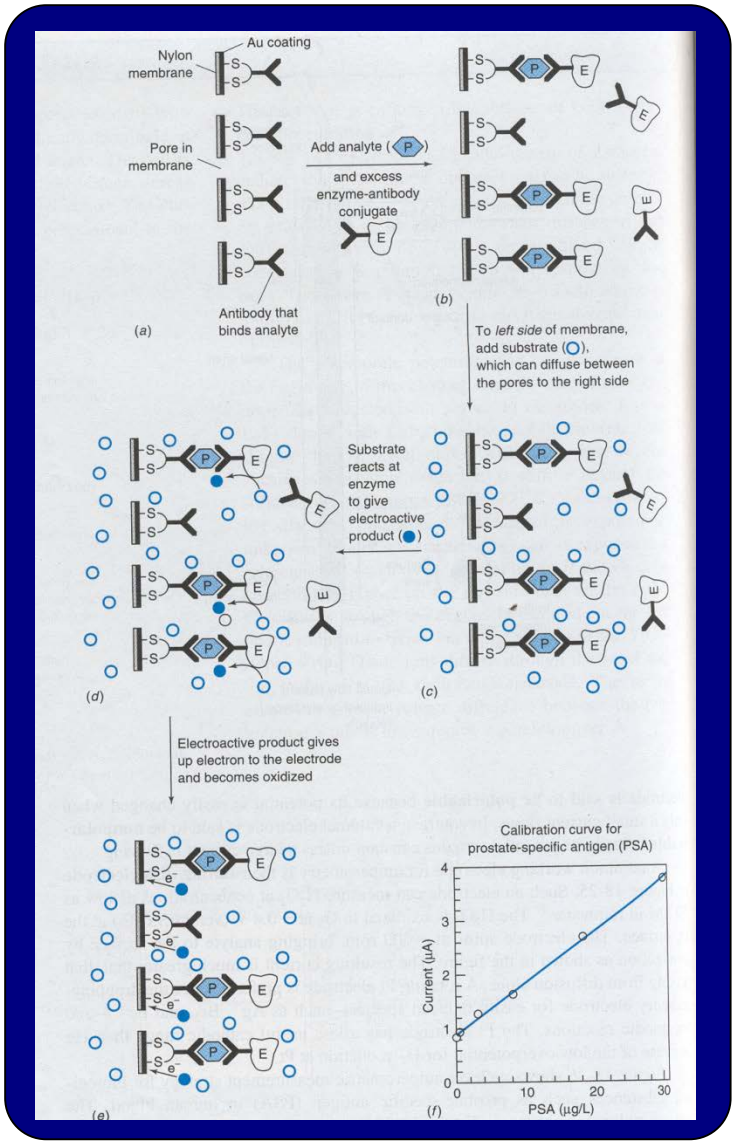

Alkaline phosphatase

- $R\text{-}OPO_3^{2-} + H_2O \rightarrow ROH + HPO_4^{2-}$

Phosphomonoester **electroactive**

Stripping Analysis

- Concentrate analyte into Hg by reduction
- Reoxidize analyte with more positive potential (anode stripping)
- Measure polarographic signal during oxidation (10^{-9} ~ 10^{-11} M)

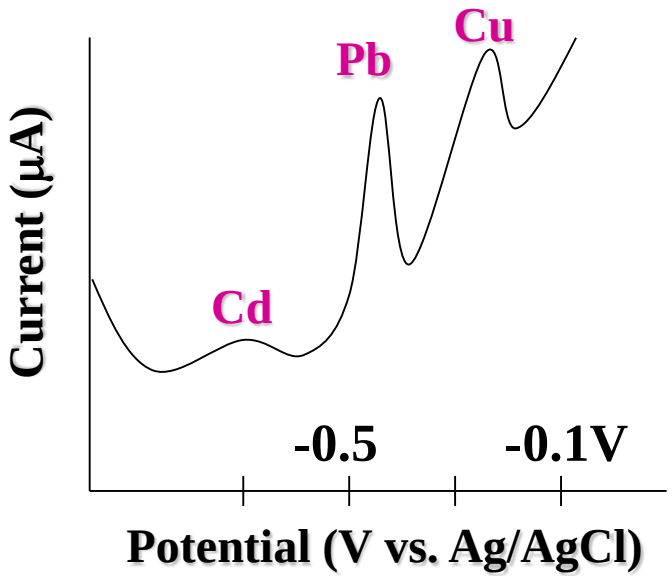

Figure 18.17 Anodic stripping voltammogram(differential pulse mode) of Sargasso seawqter acidified to pH 2. Peaks for Cd and Cu correspond to 0.02 and 1.3 mmol/kg of seawater, respectively.

Table 18.5 Detection limits for stripping analisis

Analyte	Stripping mode	Detection limit
Ag^+	Anode	$2*10^{-12}$ M
Testosterone	Anode	$2*10^{-10}$ M
I^-	Cathode	$1*10^{-10}$ M